European Journal of Medicinal Chemistry 258 (2023) 115587

Contents lists available at ScienceDirect

European Journal of Medicinal Chemistry

journal homepage: www.elsevier.com/locate/ejmech

Research paper

Development of novel PEX5-PEX14 protein-protein interaction (PPI) inhibitors based on an oxopiperazine template

Monika Marciniak [a], Piotr Mróz [a], Valeria Napolitano [b], Vishal C. Kalel [c], Roberto Fino [b], Emilia Pykacz [a], Wolfgang Schliebs [c], Oliver Plettenburg [d,e], Ralf Erdmann [c], Michael Sattler [b,f], Grzegorz M. Popowicz [b,f], Maciej Dawidowski [a,*]

[a] Department of Drug Technology and Pharmaceutical Biotechnology Medical University of Warsaw, Banacha 1, 02-097, Warszawa, Poland
[b] Institute of Structural Biology, Molecular Targets and Therapeutics Center, Helmholtz Zentrum München, Ingolstädter Landstrasse 1, 85764, Neuherberg, Germany
[c] Institute of Biochemistry and Pathobiochemistry, Department of Systems Biochemistry, Faculty of Medicine, Ruhr-University Bochum, 44780, Bochum, Germany
[d] Institute of Medicinal Chemistry, Molecular Targets and Therapeutics Center, Helmholtz Zentrum München, Ingolstädter Landstr. 1, Neuherberg, 85764, Germany
[e] Center of Biomolecular Drug Research (BMWZ), Institute of Organic Chemistry, Leibniz Universität Hannover, Schneiderberg 1b, Hannover, 30167, Germany
[f] Bavarian NMR Center, Department of Bioscience, School of Natural Sciences, Technical University of Munich, Lichtenbergstrasse 4, 85747, Garching, Germany

ARTICLE INFO

Handling Editor: Dr. Z Liu

Keywords:
Protein-protein interaction inhibitors
Peptidomimetics
α-Helical mimetics
Oxopiperazine
Trypanocidal inhibitors
Structure-based drug design

ABSTRACT

Protein-protein interactions (PPIs) constitute an important but challenging class of molecular targets for small molecules. The PEX5-PEX14 PPI has been shown to play a critical role in glycosome biogenesis and its disruption impairs the metabolism in *Trpanosoma* parasites, eventually leading to their death. Therefore, this PPI is a potential molecular target for new drugs against diseases caused by *Trypanosoma* infections. Here, we report a new class of peptidomimetic scaffolds to target the PEX5-PEX14 PPI. The molecular design was based on an oxopiperazine template for the α-helical mimetics. A structural simplification along with modifications of the central oxopiperazine scaffold and addressing the lipophilic interactions led to the development of peptidomimetics that inhibit PEX5-*Tb*PEX14 PPI and display cellular activity against *T. b. brucei*. This approach provides an alternative approach towards the development of trypanocidal agents and may be generally useful for the design of helical mimetics as PPI inhibitors.

1. Introduction

Peroxisomes are small organelles that occur in almost all eukaryotes. Although their number, morphology, protein composition and spectra of cellular functions are highly varied between the respective organisms, an important, common feature of all eukaryotic peroxisomes is that they lack DNA. Consequently, all enzymes required for their function need to be imported after being translated in the cytosol. Peroxin (PEX#) are proteins that are necessary for the biogenesis and import of peroxisomal proteins. Among many of them, PEX5, PEX13 and PEX14 play an important role in this pathway. PEX5 is the import receptor, which binds peroxisomal transport signal 1 (PTS1) peptide motifs of the matrix proteins. The cargo-loaded PEX5 is then recruited to peroxisomes with the aid of the peroxisomal membrane proteins PEX13 and PEX14 [1–5].

Trypanosoma protists use this mechanism for transporting essential metabolic enzymes into glycosomes, the peroxisome-related organelles. Consequently, blocking the peroxin-mediated glycosomal import system can lead to severe consequences for the cellular metabolism. For example, in the bloodstream form of *T. brucei* protist this would lead to the accumulation of glycosomal enzymes in the cytosol, loss of ATP and metabolic catastrophe, leading eventually to cell death. Previously, we showed that blocking the glycosomal import system by inhibition of the PEX5-PEX14 protein-protein interaction (PPI) with small molecules causes mislocalization of glycosomal enzymes, kills *T. brucei* and *T. cruzi*, thus bearing a potential as a new molecular target for the treatment of Human African Trypanosomiasis (HAT) and Chagas disease [6].

The PEX5-PEX14 PPI is mediated by a canonical α-helix of PEX5, with the indole and phenyl aromatic systems of the WxxxF/Y (where 'x' denotes any, non-proline amino acid) motif addressing the respective hydrophobic Trp and Phe/Tyr binding pockets on the surface of PEX14 (Fig. 1A) [7–10]. This PPI is characterized by a flat interface, hydrophobic, aromatic interactions, and only two shallow, solvent exposed cavities present in a large interface area, which makes it challenging to be targeted by small molecules. The previous medicinal chemistry

* Corresponding author.
E-mail address: maciej.dawidowski@wum.edu.pl (M. Dawidowski).

https://doi.org/10.1016/j.ejmech.2023.115587
Received 28 March 2023; Received in revised form 10 June 2023; Accepted 20 June 2023
Available online 25 June 2023

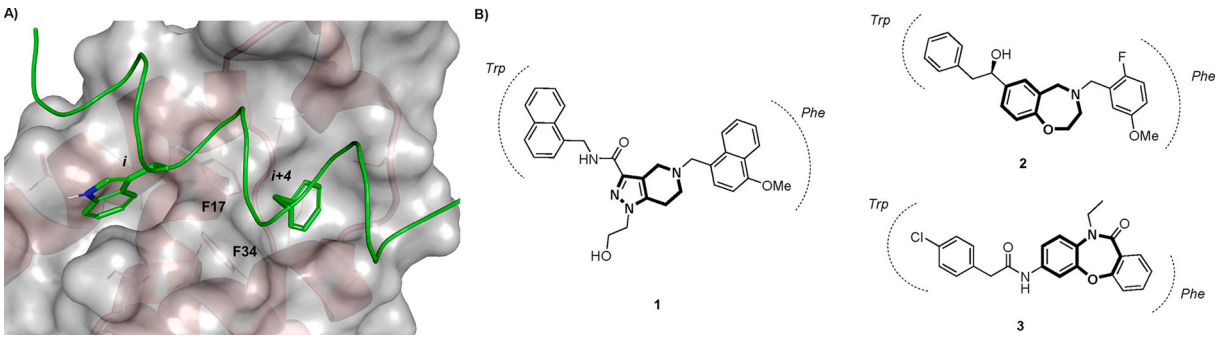

Fig. 1. A) Binding mode of PEX5 α-helix (green) to the N-terminal domain of *Hs*PEX14 (light gray, PDB accession code: 2W84). The parallel-displaced π-π stacked F17 and F34 residues of PEX14 form the Trp and a Phe pockets addressed by the respective aromatic amino acid side chains of PEX5 WxxxF motif. B) The examples of previously developed pyrazolo[4,3-*c*]pyridine **1**, 2,3,4,5-tetrahydrobenzo[*f*] [1,4]oxazepine **2** and dibenzo[*b*,*f*] [1,4]oxazepin-11(10*H*)-one **3** PEX5-PEX14 PPI inhibitors. The common binding modes are illustrated: the aromatic residues mimicking the native binding of PEX5 WxxxF fragments to PEX14 Trp and Phe pockets, and the central core (bold) shielding the solvent-exposed F17 and F34 residues.

campaigns based on the *in silico* 3D pharmacophore screening [11], the chemically advanced template search (CATS) algorithm [12] and the high-throughput screening (HTS) of a compound library [13], which led to first PEX5-PEX14 PPI inhibitor classes based on a pyrazolo[4,3-*c*] pyridine **1**, 2,3,4,5-tetrahydrobenzo[*f*] [1,4]oxazepine **2** and dibenzo[*b*, *f*] [1,4]oxazepin-11(10*H*)-one **3** scaffold, respectively (Fig. 1B). The X-ray structures and/or molecular docking results revealed, that despite these compounds belong to different chemical classes, they all possess common binding characteristics: a central core shielding the solvent-exposed F17 and F34 residues in the PEX14 interface and two aromatic moieties filling the respective Trp and Phe pockets.

PPIs are attractive molecular targets for new drugs because of their crucial role in many biochemical and signaling pathways [14]. However, due to their flat, large and solvent-exposed interfaces, and because of the absence of deep pockets for ligand binding, they are often disregarded as being challenging or even "undruggable" with drug-like scaffolds. Therefore, new strategies are investigated to inhibit formation of protein-protein complexes [15–17], many of which utilize naturally occurring peptides as templates for design of new PPI inhibitors [18–20]. As a continuation of our research on new ways to target the PEX5-PEX14 PPI, we now turn our attention to peptidomimetic scaffolds, which reproduce the spatial arrangement of the aromatic moieties of the WxxxF/Y motif of PEX5 and orient them towards their respective Trp and Phe hotspots in the PEX14 surface. Arora and co-workers showed that 2-oxopiperazine dimers derived from α-amino acids adopt stable conformations that reproduce the arrangement of *i*, *i*+*4*, and *i*+*7* residues on an 8mer canonical α-helix (Fig. 2A) [21]. Using this approach, they developed peptidomimetics they called oxopiperazine helical mimetics (OHMs) that bind MDM2-p53 and p300-HIF1*α* PPI interfaces in low- and sub-micromolar concentrations, respectively (Fig. 2B). Importantly, they showed that OHMs kill cancer cells in *in vitro* cellular assays, as well as in *vivo* tumor xenograft models. In addition, the developed oxopiperazine dimers had desirable drug-likeness properties, such as low molecular weight (MW), good solubility, high sp^3-carbon fraction and good synthetic accessibility [22,23].

All these features make OHMs a potentially useful alternative to the conventional small-molecular inhibitors targeting PPIs mediated by α-helices. Surprisingly, a literature search shows that this approach is underused and besides the recent report by Trebesco et al. on novel SARS-CoV-2 ACE2/spike interaction inhibitors [24], the 2-oxopiperazine scaffold has not been employed in design of α-helical mimetics targeting other protein complexes than MDM2-p53 and p300-HIF1*α*. In this report we investigate a novel approach of disrupting PPIs. Building on the strategy proposed by Arora and co-workers, we develop the first peptidomimetic inhibitors of the challenging PEX5-PEX14 PPI.

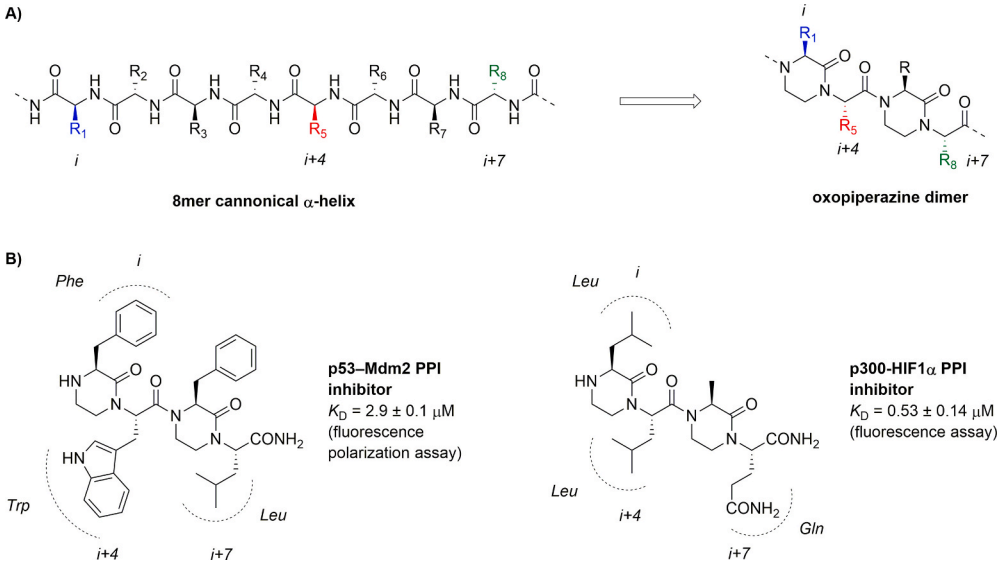

Fig. 2. Arora's approach to target PPIs with 2-oxopiperazine-based α-helical mimetics. A) Oxopiperazine dimer as a peptidomimetic scaffold that reproduces the arrangement of *i*, *i*+*4*, and *i*+*7* residues on an 8mer canonical α-helix. B) Examples of oxopiperazine dimers targeting p53-Mdm2 and p300-HIF1*α* PPI.

2. Results and discussion

2.1. Design and SAR study of oxopiperazine PEX5-PEX14 PPI inhibitors

PEX5-PEX14 PPI is mediated by the WxxxF/Y peptide motifs of the canonical α-helix of PEX5, with the indole and phenyl ring systems of Trp *i* and Phe *i+4* residues located on the same face of the helix [7]. These aromatic moieties fill the respective Trp and Phe hot-spots in the PEX14 surface. The existence of only two hot-spots mediating the protein complex formation is an important feature that differentiates this PPI from the MDM2-p53 and p300-HIF1α PPIs mediated by three binding pockets, that have been targeted by Arora and co-workers with oxopiperazine dimers. Therefore, we assumed, that in the case of PEX5-PEX14 PPI, a simplified oxopiperazine 'monomer' may be suitable for mimicking the WxxxF fragment of PEX5, without any benefit of including equivalent of *i*+7 residue present in the 2-oxopierazine dimers targeting MDM2-p53 and p300-HIF1α PPIs (Fig. 3A). This simplification potentially gives an opportunity of utilizing even lower MW inhibitors.

To support this molecular design, we overlayed a prototype 2-oxopiperazine 'monomer' **4** docked to *Tb*PEX14 with the structure of WxxxF motif of PEX5 bound to the PEX14 surface (PDB accession code: 2W84) (Fig. 3B) [7]. We observed that the positioning of the indole and phenyl moieties in their respective Trp and Phe binding pockets was similar for 2-oxopiperazine **4** and the WxxxF fragment of the native ligand PEX5.

We synthesized compound **4**, which displayed a weak PEX5-*Tb*PEX14 PPI inhibition (K_i = 265 μM), as evaluated by AlphaScreeen [25] assay. We then attempted to adjust the prototype oxopiperazine for a better fit to the *Tb*PEX14 surface using structure-based design. On closer inspection of the docking pose of **4** to *Tb*PEX14 (Fig. 3B), the phenyl ring is shifted out toward the upper rim of the Phe pocket rather than being deeply inserted into this cavity as in the case of Phe side chain of the native WxxxF motif (Fig. 3B). Our previous studies on targeting *Tb*PEX14 demonstrated that in some instances introducing a large, double aromatic system addressing the shallow Phe pocket is beneficial for the ligand binding [11]. Hence, we replaced the phenyl in **4** with a larger indole residue, which resulted in 2-oxopiperazine **5** having a two-fold improved potency in disrupting the PEX5-*Tb*PEX14 PPI (K_i = 133 μM). The analysis of the docking-derived binding mode of **5** to *Tb*PEX14 showed a more efficient filling of the Phe pocket, which facilitates stronger π-π interactions with the stacked F17 and F34 side chains of *Tb*PEX14 than in the case of the parent **4** (Fig. 4A). In addition, a distance between the carboxylate of the inhibitor and the guanidine of the R22 side chain allows for hydrogen bonding. A replacement of the ester group in **5** with a primary amide resulted in a two-fold decrease in the affinity towards *Tb*PEX14 (**6**, K_i = 288 μM). Substitution of the secondary amine in **5** with acetyl group produced derivative **7** with a significantly lower efficacy in disrupting the PEX5-*Tb*PEX14 PPI (K_i = 542 μM) compared to the parent compound.

The direct implementation of 2-oxopiperazine central core to mimic the helical WxxxF motif of PEX5 furnished only weak PEX5-*Tb*PEX14 PPI inhibitors (Table 1). To improve the ligand binding to *Tb*PEX14, we next systematically explored the possible modifications within the 2-oxopiperazine core. First, we expanded the central scaffold of **5** by one methylene unit and synthesized compound **8** with a 1,4-diazepan-2-one scaffold instead of a 2-oxopiperazine. The compound was significantly more potent in disrupting the PEX5-*Tb*PEX14 PPI (K_i = 53 μM), with respect to the parent molecule. We attributed this to an increased conformational flexibility of the 7-membered central core, which may facilitate the positioning of the hydrophobic aromatic rings of the compound in their respective binding pockets in the *Tb*PEX14 surface (Fig. 4B). Next, we investigated the 2-oxopiperazine analogs with various carbonyl positions in the central scaffold. The piperazine-2,5-dione derivatives **9** and **10** of compound **4** did not inhibit PEX5-*Tb*PEX14 PPI (K_i > 1000 μM, for both). Changing the carbonyl position in **4** and **5** produced the respective analogs **11** and **12**. Propitiously, both derivatives displayed a markedly higher potency in inhibition of PEX5-*Tb*PEX14 PPI (K_i = 73 and 27 μM, respectively), than that of the parent compounds. Comparison of the docking-derived binding modes of compounds **5** and **12** shows a very similar positioning of their aromatic residues in the corresponding binding pockets in *Tb*PEX14 (Fig. 4A and C, respectively). Therefore, it seems that the observed differences in the activities of these compounds are caused by the unfavorable position of the carbonyl oxygen in **5**, which is in close proximity of the F34 residue in *Tb*PEX14. However, other factors may contribute to ligand binding to the flat, solvent-exposed surfaces. For example, our previous works on the pyrazolo[4,3-*c*]pyridine PEX5-PEX14 PPI inhibitors similar to **1** (Fig. 1B) showed that the positively charged nitrogen of the ligand proximal to the upper rim of the Phe pocket in *Tb*PEX14 plays an important role in facilitating the solvent network around the ligand-protein complex [26]. The tertiary amine nitrogen in **12** adopts a similar orientation, which may explain the higher activity of the compound, as compared to **5**. The 2,3-dioxo analog **13** of 2-oxopiperazine **5** displayed a stronger inhibition of PEX5-*Tb*PEX14 PPI (K_i = 75 μM), with respect to the parent molecule, albeit its activity was lower than this of compound **12**.

Replacement of the carboxylate group in **5** by a primary carboxamide led to compound **6** displaying a notable decrease in inhibiting PEX5-*Tb*PEX14 complex formation. To learn more about the importance of the C-terminal carboxylate, we performed further structure−activity relationship studies using the oxopiperazine template present in compounds **11** and **12**. First, we synthesized compounds **14** and **15**, the alcohol and acetoxy derivatives of **12**. Both compounds displayed a two-fold lower activity in disrupting PEX5-*Tb*PEX14 PPI (K_i = 48 and 58 μM, respectively), than the parent **12**. Next, we synthesized compound **16**, a derivative of **12** without a C-terminal functional group. The compound was less active (K_i = 41 μM) than the parent molecule. We also obtained

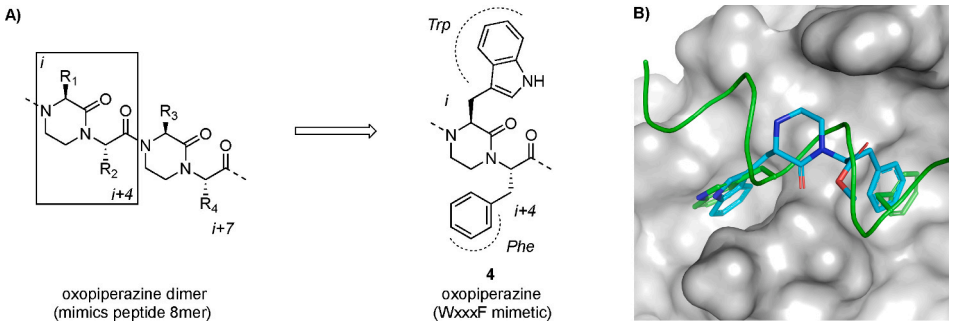

Fig. 3. A) Design of a prototype oxopiperazine WxxxF mimetic **4** as PEX5-PEX14 PPI inhibitor. B) Comparison of the docked pose of compound **4** (blue) to *Tb*PEX14 (gray) and the structure of WxxxF PEX 5 motif (green) bound to *Tb*PEX14 surface (PDB accession code: 2W84). The positions of the aromatic residues addressing the respective Trp and Phe pockets of PEX14 are similar in **4** and WxxxF fragment.

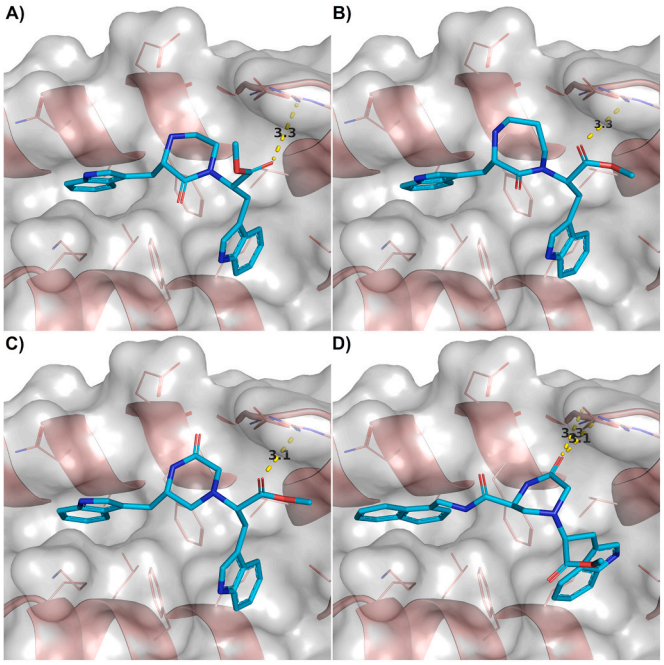

Fig. 4. Docking-derived binding models of **5** (A), **8** (B), **12** (C) and **19** (D) to PEX5-*Tb*PEX14 PPI interface.

Table 1
Primary design: activity of compounds **4**–**7** against *Tb*PEX5-PEX14 PPI, *T. b. brucei* and *HepG2* cells.

#	Formula[a]	*Tb*PEX14 K_i [μM][b]	*T. b. brucei* EC_{50} [μM][c]	*HepG2* EC_{50} [μM][c]	SI[d]
4	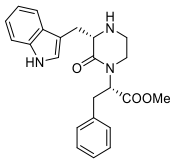	265 ± 15	43 (33–54)	>100	>2.3
5	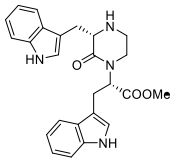	133 ± 4	30 (23–37)	>100	>3.4
6	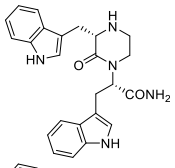	288 ± 11	>100	>100	–
7	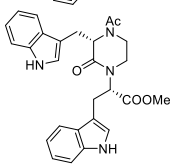	542 ± 46	>100	>100	–
1		5 ± 1	4 (3–4)[e]	>50[e]	>14

[a] Chemical structure of **1** is shown in Fig. 1B.
[b] Values were calculated as a Hill curve fit to 12-point titration. The values are shown as mean (n = 4).
[c] Values are shown as mean (n = 4). Values in parentheses are 95% confidence intervals.
[d] Selectivity index is calculated as HepG2 EC_{50} [μM]/*T. b. brucei* EC_{50} [μM].
[e] Data taken from Ref. [6].

derivative **17** in which the indole residue addressing the Phe pocket was linked to the oxopiperazine framework through an amide bond. The activity of both compound was significantly lower (K_i = 195 μM), when compared to the structurally related derivative **12**.

In the pyrazolo[4,3-*c*]pyridine series of PEX5-*Tb*PEX14 PPI inhibitors described previously, the aromatic residue addressing the Trp pocket in *Tb*PEX14 was linked to the central scaffold through a carboxamide bond. We have shown, that such arrangement favors an important through-water binding to the hydrophilic amino-acid side chains of the *Tb*PEX14 surface and thus plays an important role in creating the water envelope around the ligand-protein complex [11,13,26]. Hence, we decided to verify if a similar design can be adapted for optimization of the oxopiperazine series and synthesized derivatives **18** and **19**. The results of molecular docking suggest a different binding mode of these analogs than that of the other 2-oxopiperazine PEX5-*Tb*PEX14 PPI inhibitors (Fig. 4D). Compound **18** displayed a modest activity (K_i = 494 μM). The naphthyl analog **19** was markedly more potent (K_i = 77 μM), however at the cost of a significantly increased hydrophobicity. Despite the limited utility of **18** and **19** as PEX5-*Tb*PEX14 PPI inhibitors, they are based on the unpreceded (*S*)-6-oxopiperazine-2-carboxylate scaffold with a C-terminal α-amino acid residue attached to the N-4 atom, which can be useful for design of novel peptidomimetics [27].

2.2. NMR validation experiment

To validate the binding mode of 2-oxopiperazines to *Tb*PEX14 surface, compound **12** was tested in a NMR ^{1}H-^{15}N 2D heteronuclear single-quantum coherence correlation experiment. The compound interacted with the N-terminal domain of *Tb*PEX14 in fast exchange on the NMR chemical shift time scale (Fig. S1 in supplementary data). The NMR spectra show that some of the affected resonances are attributable to assigned residues near the binding site for the PEX5 WxxxF motif. This indicates compound **12** binds at the binding site expected on the basis of the docking pose generated (Fig. 4C).

2.3. Cellular activity of oxopiperazine PEX14–PEX5 PPI inhibitors

Having investigated the structure-activity relationship of oxopiperazine PEX5-*Tb*PEX14 PPI inhibitors, we next sought to determine if the developed compounds possess *in vitro* cellular activity and whether this activity correlates with the potency in disrupting the PEX5-*Tb*PEX14 PPI evaluated in AlphaScreen assay. We tested the compounds for their trypanocidal activity using *T. b. brucei* bloodstream form parasites as the model organism employing peroxisomal import to maintain the crucial life functions. In addition, we determined the cytotoxicity of the compounds in HepG2 (hepatocyte) cells. The results are presented in Tables 1–4. In general, we observed a good correlation between the potency in disrupting the PEX5-*Tb*PEX14 complex formation and the activity against *T. b. brucei*. The PEX5-*Tb*PEX14 PPI inhibitors **4**, **5**, **8**, **11**, **12**, **16**, **19** displayed trypanocidal activities in micromolar concentrations whereas the derivatives **6**–**7**, **10**, **17** and **18** with low activities in the AlphaScreen assay did not kill *T. b. brucei*. Compound **9** was the only exception form this trend, showing a modest trypanocidal activity accompanied by an unspecific cytotoxicity. Most of the tested inhibitors showed selectivity between antiparasitic activity and cytotoxicity against HepG2 cells. Compounds **8** and **12** were most potent against bloodstream form of *T. b. brucei*, displaying low-micromolar EC_{50} values comparable to those observed for **1** [6] and some other PEX5-*Tb*PEX14 PPI inhibitors studied previously [12,13].

2.4. Chemistry

The (*S*)-3-((1*H*-indol-3-yl)methyl)piperazin-2-one and (*S*)-3-((1*H*-indol-3-yl)methyl)-1,4-diazepan-2-one peptidomimetics **4**–**8** were synthesized employing a Fukuyama–Mitsunobu cyclization strategy [28] as

Table 2
Modifications of the central scaffold: activity of compounds **8**–**13** against *Tb*PEX5-PEX14 PPI, *T. b. brucei* and *HepG2* cells.

#	Formula[a]	*Tb*PEX14 K_i [μM][b]	*T. b. brucei* EC_{50} [μM][c]	*HepG2* EC_{50} [μM][c]	SI[d]
8	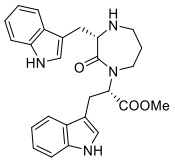	53 ± 2	5 (4–6)	21 (15–25)	4.2
9	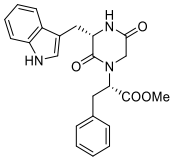	>1000	29 (24–35)	24 (15–39)	<1
10	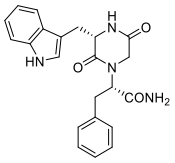	>1000	>100	>100	–
11	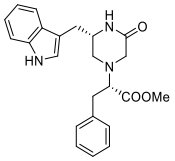	73 ± 2	13 (8–18)	56 (37–121)	4.3
12	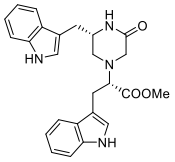	27 ± 1	5 (4–6)	17 (15–19)	3.6
13	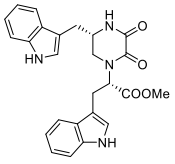	75 ± 3	29 (22–38)	>100	>3.4
1		5 ± 1	4 (3–4)[e]	>50[e]	>14

[a] Chemical structure of **1** is shown in Fig. 1B.
[b] Values were calculated as a Hill curve fit to 12-point titration. The values are shown as mean (n = 4).
[c] Values are shown as mean (n = 4). Values in parentheses are 95% confidence intervals.
[d] Selectivity index is calculated as HepG2 EC_{50} [μM]/*T. b. brucei* EC_{50} [μM].
[e] Data taken from Ref. [6].

a key step, as shown in Schemes 1 and 2. L-H-Trp-OH was esterified with MeOH and the amine group of the resulting ester **20** was acylated with *o*-NsCl to give the sulfonamide **21**, that upon hydrolysis yielded carboxylate **22**. Peptide coupling with L-H-Phe-OMe or L-H-Trp-OMe followed by Mitsunobu reaction of the respective products **23** and **24** with 2-bromoethanol provided the acyclic precursors of piperazin-2-one **25** and **26**. In a similar manner, **24** was reacted with 3-bromopropanol to provide the 1,4-diazepan-2-one precursor **27**. The subsequent DBU-triggered cyclocondensation reactions of bromides **25**–**27** followed by the Ns-deprotection of the respective 2-oxopiperazines **28**–**30** led to the target products **4**, **5**, **8**. Amide **6** was obtained from ester **5** by aminolysis. Alternatively, the secondary amine of **5** was acetylated to give the tertiary amide **7**.

(*S*)-3-((1*H*-indol-3-yl)methyl)piperazine-2,5-dione derivatives **9** and **10** were synthesized as shown in Scheme 3. L-Boc-Trp-OH was coupled with L-H-Phe-OMe using TBTU activation. The obtained intermediate **31**

Table 3
Modifications of the C-terminus: activity of compounds **14**–**17** against *Tb*PEX5-PEX14 PPI, *T. b. brucei* and *HepG2* cells.

#	Formula[a]	*Tb*PEX14 K_i [μM][b]	*T. b. brucei* EC_{50} [μM][c]	*HepG2* EC_{50} [μM][c]	SI[d]
14	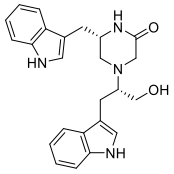	48 ± 2	14 (12–16)[e]	24 (16–37)	1.7
15	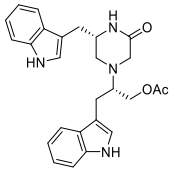	58 ± 1	13 (11–6)	29 (24–35)	1.8
16	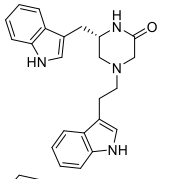	41 ± 2	7 (6–9)	12 (6–22)	1.7
17	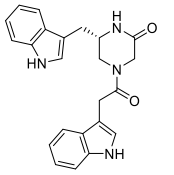	195 ± 4	>100	>100	–
1		5 ± 1	4 (3–4)[e]	>50[e]	>14

[a] Chemical structure of **1** is shown in Fig. 1B.
[b] Values were calculated as a Hill curve fit to 12-point titration. The values are shown as mean (n = 4).
[c] Values are shown as mean (n = 4). Values in parentheses are 95% confidence intervals.
[d] Selectivity index is calculated as HepG2 EC_{50} [μM]/*T. b. brucei* EC_{50} [μM].
[e] Data taken from Ref. [6].

Table 4
Activity of compounds **18**–**19** against *Tb*PEX5-PEX14 PPI, *T. b. brucei* and *HepG2* cells.

#	Formula[a]	*Tb*PEX14 K_i [μM][b]	*T. b. brucei* EC_{50} [μM][c]	*HepG2* EC_{50} [μM][c]	SI[d]
18	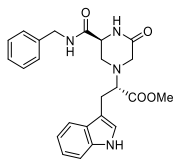	494 ± 34	>100	>100	NA
19	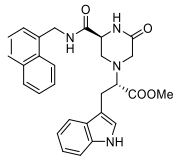	77 ± 3	10 (9–12)	33 (31–36)	3.2
1		5 ± 1	4 (3–4)[e]	>50[e]	>14

[a] Chemical structure of **1** is shown in Fig. 1B.
[b] Values were calculated as a Hill curve fit to 12-point titration. The values are shown as mean (n = 4).
[c] Values are shown as mean (n = 4). Values in parentheses are 95% confidence intervals.
[d] Selectivity index is calculated as HepG2 EC_{50} [μM]/*T. b. brucei* EC_{50} [μM].
[e] Data taken from Ref. [6].

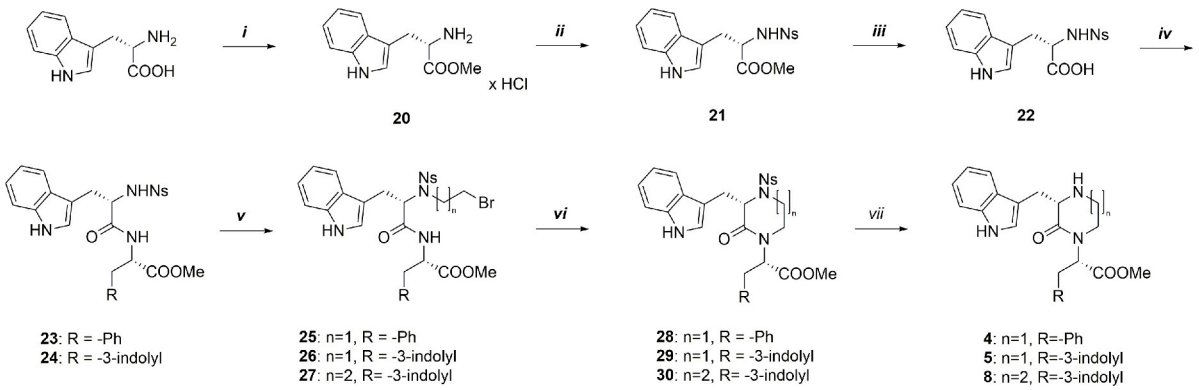

Scheme 1. *i.* $SOCl_2$, MeOH, reflux; *ii. o*-NsCl, TEA, DMAP, DCM, 0 °C to rt; *iii.* LiOH, TEA, water, rt; *iv.* L-H-Phe-OMe or L-H-Trp-OMe, EDC, HOBt, DIPEA, DCM, 0 °C to rt; *v.* 2-bromoethanol or 3-bromopropanol, DEAD, PPh_3, THF, 0 °C to rt; *vi.* DBU, THF, rt; *vii.* PhSH, Cs_2CO_3, DMF, rt.

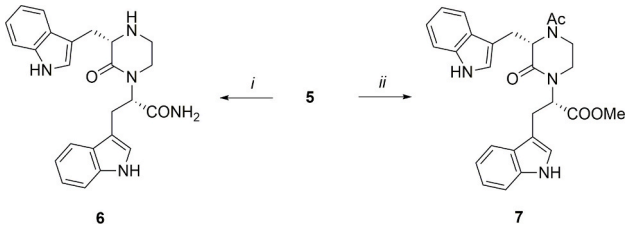

Scheme 2. *i.* NH_3, MeOH, reflux. *ii.* Ac_2O, DIPEA, DMAP, DCM, 0 °C to rt.

was subjected to Boc-cleavage under acidic conditions and the resulting free amine was acylated with bromoacetyl chloride to give the acyclic piperazine-2,5-dione precursor **32**. The intramolecular amide *N*-alkylation afforded the cyclic **9** bearing a terminal Phe-OMe, which was subsequently converted into the corresponding amide **10** by treatment with concentrated methanolic ammonia.

The (*S*)-6-((1*H*-indol-3-yl)methyl)piperazin-2-one-based peptidomimetics **11** and **12**, having the C-terminal Phe-OMe and Trp-OMe residues, respectively, were synthesized as shown in Scheme 4. L-H-Trp-OH was reduced with LAH followed by amine protection with Boc group. The resulting L-Boc-Trp-ol **33** was oxidized to L-Boc-Trp-al **34** under the Parikh–Doering conditions [29,30]. The aldehyde **34** was subjected to reductive amination with L-H-Phe-OMe or L-H-Trp-OMe to provide the amines **35** and **36**, respectively, which were then *N*-alkylated with ethyl bromoacetate. The obtained products **37** and **38** were Boc-deprotected in acidic conditions/cyclized to the respective target 2-piperazinones **11** and **12**. A side reaction of cyclocondensation employing a more hindered carbonyl occurred, which resulted in a formation of products **39** and **40**.

All attempts to obtain the alcohol **14** by reduction of ester **12** using various conditions and reagents including $LiBH_4$ failed. Hence, **14** was synthesized from **34** using a reductive amination/deprotection/cyclocondensation sequence, as shown in Scheme 5. **34** was subjected to reductive amination with L-Trp-ol to provide the amine **41**. The subsequent *N*-alkylation reaction with ethyl bromoacetate gave the amino esters **42** along with its lactone derivative **43**. Removal of the Boc protecting group in **42** followed by cyclization yielded the target oxopiperazine **14**. Acetylation of the primary alcohol in **14** provided **15**.

The (*S*)-5-((1*H*-indol-3-yl)methyl)piperazine-2,3-dione derivative **13** was synthesized by *N*-Boc deprotection of **36**, followed by *N*-acylation and subsequent cyclocondensation of the resulting amino ester **44** in presence of TEA, as shown in Scheme 6.

Compounds **16** and **17** were synthesized as shown in Scheme 7. Aldehyde **34** was subjected to reductive amination with Gly-OMe, followed by a deprotection-cyclization sequence of the resulting amino ester **45** to give 2-oxopiperazine **46**. Reductive amination or EDC-mediated acylation of **46** gave the final derivatives **16** and **17**, respectively.

The (*S*)-6-oxopiperazine-2-carboxamide derivatives **18** and **19** were synthesized as shown in Scheme 8. First, L-Boc-Ser-OBn was reacted

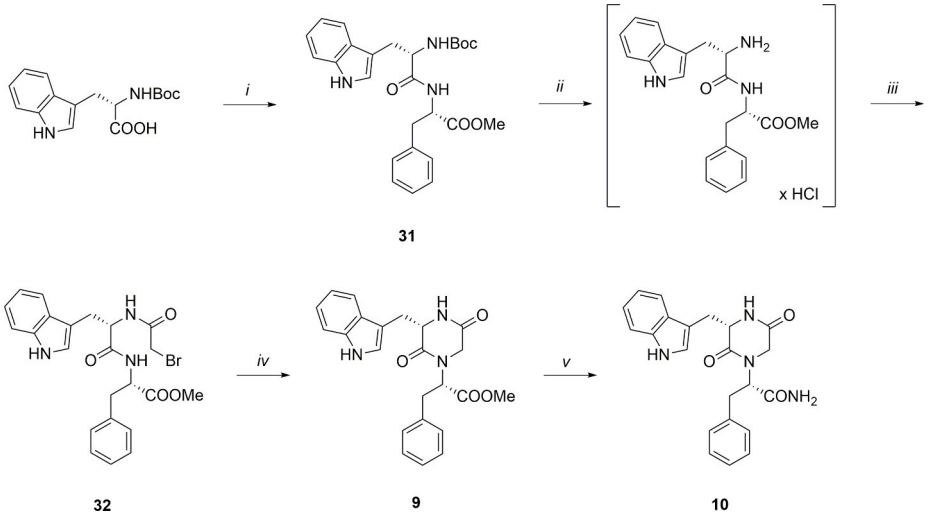

Scheme 3. *i.* L-H-Phe-OMe TBTU, DIPEA, DMF, 0 °C to rt; *ii.* 4 N HCl, 1,4-dioxane, rt; *iii.* bromoacetyl bromide, DIPEA, DMAP, DCM, 0 °C to rt; *iv.* Cs_2CO_3, DMF, rt.; *v.* NH_3, MeOH, rt.

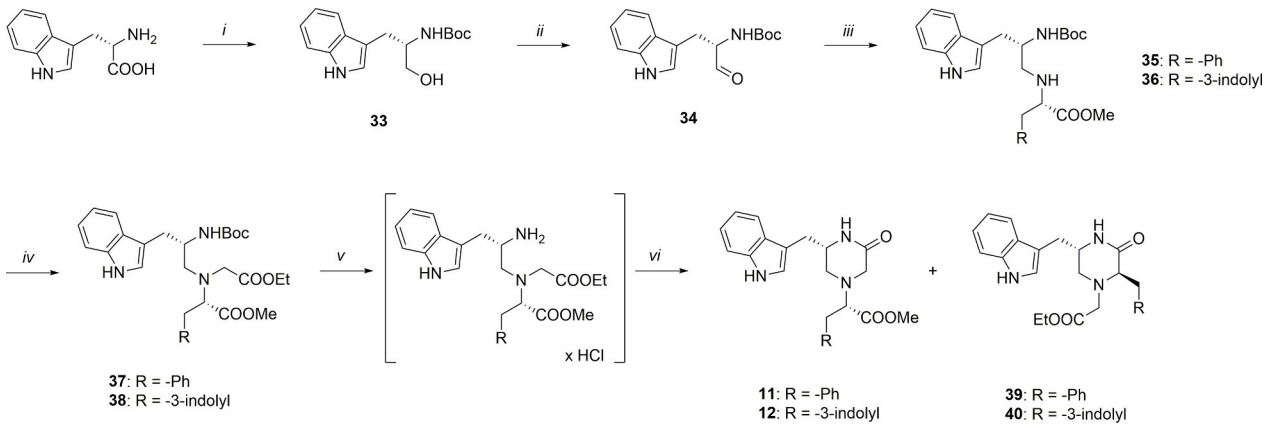

Scheme 4. *i.* LAH, THF, 0 °C to rt, then $(Boc)_2O$, THF, H_2O, rt; *ii.* $PySO_3$, TEA, DMSO, rt; *iii.* L-H-Phe-OMe or L-H-Trp-OMe, $NaBH(OAc)_3$, THF, rt; *iv*. Ethyl bromoacetate, DIPEA, CH_3CN, 70 °C; *v*. 4 N HCl, 1,4-dioxane, rt; *vi*. TEA, MeOH, rt.

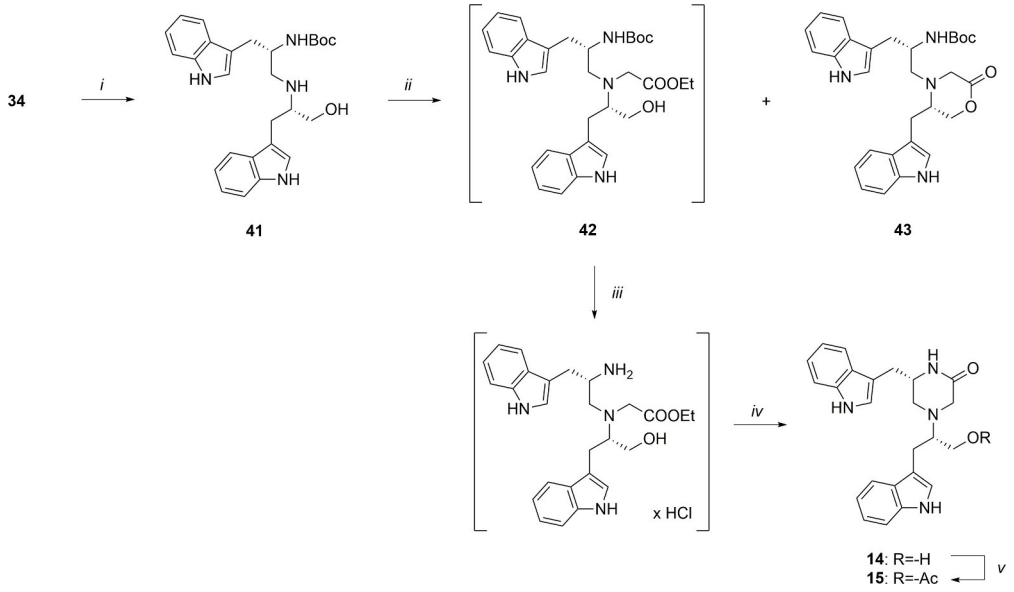

Scheme 5. *i.* L-H-Trp-ol, $NaBH(OAc)_3$, THF, rt; *ii*. Ethyl bromoacetate, DIPEA, CH_3CN, 70 °C; *iii.* 4 N HCl, 1,4-dioxane, rt; *iv*. TEA, MeOH, rt; *v*. Ac_2O, DIPEA, DMAP, DCM, 0 °C to rt.

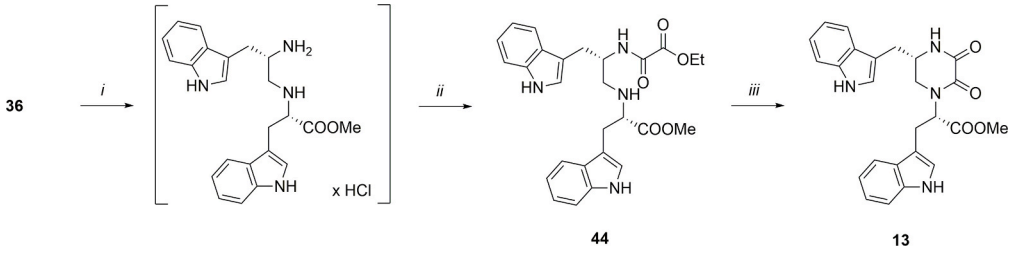

Scheme 6. *i.* 4 N HCl, 1,4-dioxane, rt; *ii.* $(COOEt)_2$, TEA, EtOH, reflux; *iii*. toluene, TEA, reflux.

with $SOCl_2$ in the presence of a base to give a cyclic sulfamidite, which was then oxidized with $NaIO_4/RuCl_3$ to the cyclic sulfamidate **47**. Intermediate **48** was obtained by N-alkylation of L-H-Trp-OMe with methyl bromoacetate. The cyclic (*S*)-6-oxopiperazine-2-carboxylate **49** was assembled by a three-step procedure comprising the N-alkylation of **48** with sulfamidate **47**, HCl-mediated one-pot Boc-deprotection/sulfamate cleavage and intramolecular aminolysis. The obtained ester **49** was then deprotected by transfer hydrogenation employing 1,4-cyclohexadiene and Pd/C catalyst. Finally, **18** and **19** were synthesized from carboxylate **50** by EDC/HOBt-mediated coupling with benzylamine and 1-naphthylmethylamine, respectively.

3. Conclusions

Despite a constant progress in development of PPI inhibitors, this class of therapeutics remains to be difficult to target by small-molecules. Therefore, there is a considerable interest to identify alternative chemical matter to furnish new leads with desirable activity. Peptidomimetics

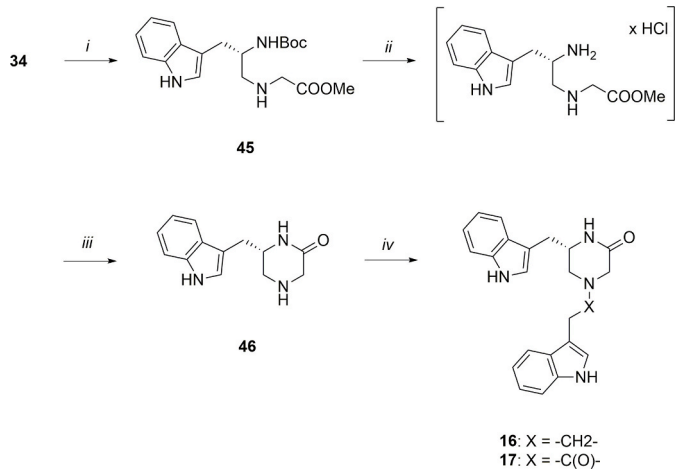

Scheme 7. *i.* Gly-MeOxHCl, $NaBH_3CN$, AcOH, DCM/MeOH, rt; *ii.* 4 N HCl, 1,4-dioxane, rt; *iii.* 3-indoleacetaldehyde, $NaBH(OAc)_3$, THF, rt (for **16**) or TEA, MeOH, rt; *iv.* 3-indoleacetic acid, EDC, DIPEA, DMAP, DMF, 0 °C to rt (for **17**).

have long been recognized as attractive tools to modulate PPIs. In this study, we adopted a strategy based on oxopiperazine α-helical mimetics proposed by Arora and co-workers to target the challenging PEX5-PEX14 PPI. Using a combination of ligand- and structure-based approach we have designed a novel class of compounds that inhibit the PEX5-PEX14 PPI at mid- and low-micromolar concentrations. A systematic re-modelling of the central 2-oxopiperazine core of the initially designed compound **4** and addressing hydrophobic interactions in the Phe pocket in PEX14 resulted in a considerable increase of activity. Derivative **12** emerged as most potent compound from the oxopiperazine series. In addition, the 1,4-diazepan-2-one framework represented by compound **8** may be considered a valuable scaffold for development of PEX14-PEX5 PPI inhibitors, which will be investigated in more details in the future. Importantly, the developed inhibitors were active in cellular system, some of them showing a low-micromolar trypanocidal activity against *T. brucei*. The activity profiles of the developed agents are comparable to some of the previously developed PEX5-PEX14 PPI inhibitors, therefore they constitute interesting starting points for future optimization. In addition, we believe that the presented design is not only useful for development of next generation of PEX5-PEX14 PPI inhibitors, but is a valuable extension of the strategy proposed by Arora and co-workers and has a potential applicability in development of peptidomimetics against other molecular targets.

4. Experimental section

4.1. Chemistry

If not noted otherwise, all reactions in non-protic solvents were carried out under argon atmosphere in oven dried glassware with magnetic stirring. Commercially available chemicals were used without further purification. Dry solvents (THF, DMF, CH_2Cl_2) were purchased from Acros Organics. Thin Layer Chromatography (TLC) was carried out on Merck TLC Silica gel 60 glass plates. Manual flash column chromatography (CC) was performed using Merck Silica gel 60 (particle size 0.040–0.063 mm, 230–400 mesh ASTM). Automated CC was performed on a Buchi Reveleris Prep purification system using Buchi Reveleris or Silicycle Silasep silica cartridges for normal phase (SiO_2) and Buchi Reveleris or Silicycle Silasep C-18 cartridges for reverse-phase (RP-C18) separations. LC-MS analyses performed on an Agilent 1220 Infinity II Gradient LC System coupled with an Agilent LC/MSD single-quadrupole detector (column: Poroshell 120, EC-C18, 3.0 × 50 mm, 2.7 μm; gradient: water/MeCN containing 0.1% (v/v) formic acid each, 5–95% MeCN; UV detection at 220 and 254 nm). High resolution mass spectrometry (HRMS) analyses were carried out using a Thermo Scientific Q-Exactive apparatus using an electrospray ionization (ESI). NMR data were recorded on a Varian 300 MHz VNMRS, Agilent 400-MR DD2 400 MHz, Bruker Avance III HD 400 or Varian Inova 500 MHz instruments. NMR peaks are reported as follows: chemical shift (δ) in parts per million (ppm) relative to residual non-deuterated solvent and/or tetramethylsilane (TMS) as the internal standards. The resonance signals are described in the following order: multiplicity, coupling constant (in Hz) and integration. The final compounds **4**–**19** were ≥95% pure, as determined by ^{1}H NMR and/or by LC-MS.

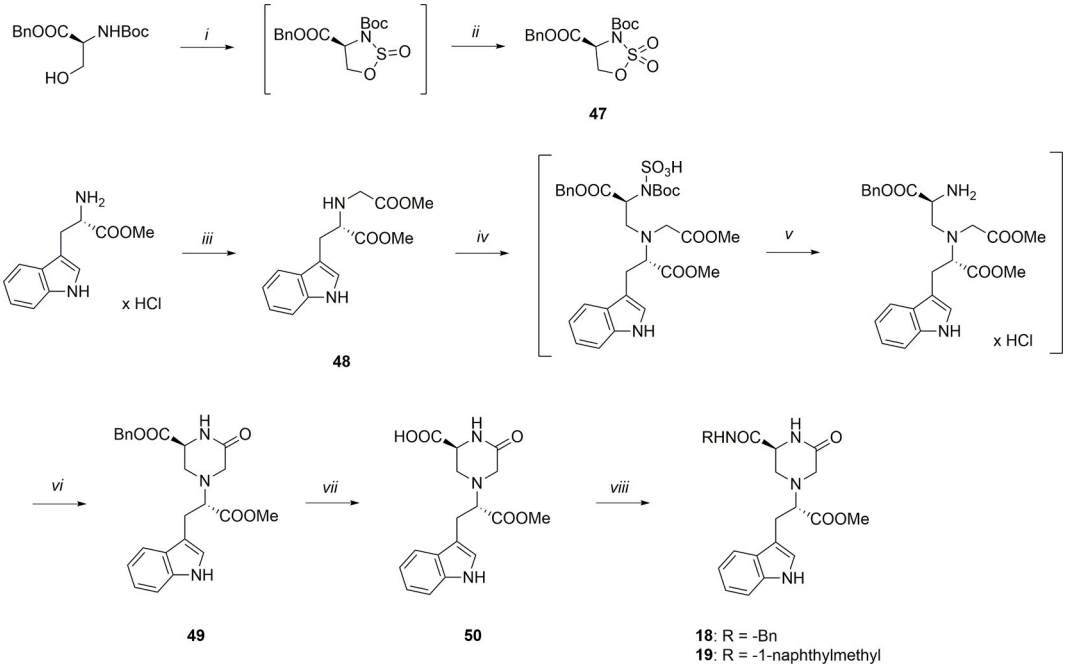

Scheme 8. *i.* $SOCl_2$, imidazole, CH_2Cl_2, -78 °C to rt; *ii.* $NaIO_4$, $RuCl_3$, CH_3CN, water, 0 °C to rt; *iii.* methyl bromoacetate, DIPEA, CH_3CN, rt; *iv.* **50**, CH_3CN, 70 °C; *v.* 4 N HCl, 1,4-dioxane, rt; *vi.* TEA, MeOH, rt; *vii.* 1,4-cyclohexadiene, 10% Pd/C, MeOH, reflux; *viii.* $BnNH_2$ or 1-naphthylmethylamine, EDC, HOBt, DIPEA, DMF, rt.

4.2. Methyl L-tryptophanate hydrochloride **20**

A slurry of L-H-Trp-OH (67.00 g, 328.1 mmol) in dry MeOH (500 mL) was cooled (−5 °C). $SOCl_2$ (47.65 mL, 2.0 eq., 656.1 mmol) was added slowly with constant vigorous stirring at such rate that the reaction temperature does not exceed 10 °C. The mixture was stirred at room temperature overnight and the obtained solid was filtered, washed with cold MeOH and *n*-hexanes, dried to give **20** (67.88 g, 81%). White solid; LC-MS (*m/z*): 219 $[M+H]^+$.

4.3. Methyl ((2-nitrophenyl)sulfonyl)-L-tryptophanate **21**

A slurry of **20** (35.00 g. 137.4 mmol) and DMAP (0.84 g, 0.05 eq., 6.9 mmol) in dry DCM (300 mL) was cooled (0 °C) and TEA (38.33 mL, 2.0 eq., 274.8 mmol) was added slowly. To this suspension was added *o*-NsCl (30.45 g, 1.0 eq., 137.4 mmol) portionwise and the resulting mixture was allowed to reach rt and stirred overnight. 1 M aqueous solution of citric acid (200 mL) was added and the mixture was shaken in a separatory funnel. The layers were separated and the aqueous phase was washed with CH_2Cl_2 (3 × 75 mL). The combined organic extracts were washed with water (100 mL), saturated aqueous solution of $NaHCO_3$ (100 mL) and saturated aqueous solution of NaCl (100 mL), dried over anhydrous Na_2SO_4, filtered and evaporated *in vacuo*. The residue was crystalized from MeOH and the resulting solid was washed with *n*-hexanes and dried to give **21** (50.03 g, 90%). Yellow solid; ^{1}H NMR (300 MHz, $CDCl_3$) δ 8.07 (bs, 1H), 7.92–7.83 (m, 1H), 7.73–7.63 (m, 1H), 7.53 7.60–7.45 (m, 2H), 7.38 (d, J = 7.9 Hz, 1H), 7.25 (d, J = 8.2 Hz, 1H), 7.12 (ddd, J = 8.1, 7.0, 1.2 Hz, 1H), 7.06 (d, J = 2.4 Hz, 1H), 6.99 (ddd, J = 8.0, 7.0, 1.1 Hz, 1H), 6.03 (d, J = 7.6 Hz, 1H), 4.48 (td, J = 7.5, 5.1 Hz, 1H), 3.56 (s, 3H), 3.35 (dd, J = 14.8, 5.1 Hz, 1H), 3.24 (dd, J = 14.7, 7.5 Hz, 1H); ^{13}C NMR (75 MHz, $CDCl_3$) δ 171.4, 147.0, 136.2, 133.7, 133.3, 132.7, 130.2, 126.7, 125.4, 123.8, 122.2, 119.8, 118.3, 111.4, 108.7, 56.8, 52.6, 29.0; LC-MS (*m/z*): 404 $[M+H]^+$.

4.4. ((2-Nitrophenyl)sulfonyl)-L-tryptophan **22**

Compound **21** (58.40 g, 132.8 mmol) was dissolved in THF (400 mL) and a solution of LiOH x H_2O (18.22 g, 3.0 eq., 398.3 mmol) in water (100 mL) was added. The mixture was vigorously stirred for 4 h. THF was evaporated *in vacuo* and the residue was stirred vigorously with a DCM and MeOH (8:1, 300 mL). The mixture was acidified with 33% aqueous solution of HCl keeping the temperature below 20 °C by external cooling with a mixture of ice and water. The layers were separated in separatory funnel and the aqueous phase was extracted with DCM and MeOH (8:1, 4 × 100 mL). The combined organic extracts were washed with water (2 × 75 mL), dried over anhydrous Na_2SO_4, filtered and evaporated *in vacuo* to give **22** (50.23 g, 90%). Light-brown solid; ^{1}H NMR (300 MHz, $CDCl_3$) δ 8.02 (bs, 1H), 7.91–7.82 (m, 1H), 7.68–7.59 (m, 1H), 7.56–7.44 (m, 2H), 7.38 (d, J = 7.9 Hz, 1H), 7.30–7.21 (m, 1H), 7.19–7.06 (m, 2H), 6.97 (t, J = 7.5 Hz, 1H), 6.01 (d, J = 7.0 Hz, 1H), 4.53–4.41 (m, 1H), 3.41 (dd, J = 14.7, 4.9 Hz, 1H), 3.24 (dd, J = 14.8, 7.9 Hz, 1H); ^{13}C NMR (75 MHz, $CDCl_3$) δ 174.7, 146.8, 136.2, 133.5, 133.2, 132.8, 130.3, 126.6, 125.5, 124.0, 122.4, 119.9, 118.3, 111.3, 108.5, 56.5, 28.8; LC-MS (*m/z*): 390 $[M+H]^+$.

4.5. Methyl ((4-nitrophenyl)sulfonyl)-L-tryptophyl-L-phenylalaninate **23**

A solution of **22** (4.00 g, 10.27 mmol) in DMF (100 mL) is cooled (0 °C), followed by the addition of EDC (3.54 g, 1.2.eq., 18.49 mmol), HOBt (2.08 g, 1.5 eq., 15.41 mmol), L-H-Phe-OMe x HCl (2.22 g, 1.0 eq., 10.27 mmol) and DIPEA (5.37 mL, 3.0 eq., 30.82 mmol). The mixture was allowed to reach rt and stirred overnight. AcOEt (120 mL) and water (150 mL) were added and the mixture was shaken in a separatory funnel. The layers were separated and the aqueous phase was extracted with EA (50 mL). The combined organic extracts were washed with 1 M aqueous solution of citric acid (50 mL), water (50 mL), saturated aqueous solution of $NaHCO_3$ (50 mL), water (50 mL) and saturated aqueous solution of NH_4Cl (5 × 40 mL), dried over anhydrous Na_2SO_4, filtered and evaporated *in vacuo*. The residue was subjected to CC (manual, SiO_2, *n*-hexane/AcOEt 3:1 to 1:2) to give **23** (4.50 g, 80%). Beige solid; ^{1}H NMR (500 MHz, $CDCl_3$) δ 8.09 (bs, 1H), 7.76 (dd, J = 7.8, 1.6 Hz, 1H), 7.47 (dd, J = 7.9, 1.4 Hz, 1H), 7.37 (td, J = 7.7, 1.6 Hz, 1H), 7.31 (td, J = 7.6, 1.4 Hz, 1H), 7.29–7.18 (m, 4H), 7.13 (d, J = 8.1 Hz, 1H), 7.11 (d, J = 7.9 Hz, 1H), 7.09–7.05 (m, 2H), 7.03 (ddd, J = 8.1, 7.0, 1.1 Hz, 1H), 6.99 (d, J = 2.4 Hz, 1H), 6.83 (ddd, J = 7.9, 7.0, 1.0 Hz, 1H), 6.02 (bs, 1H), 4.88 (ddd, J = 7.9, 6.9, 5.8 Hz, 1H), 4.14–4.07 (m, 1H), 3.71 (s, 3H), 3.32 (dd, J = 14.9, 4.8 Hz, 1H), 3.16 (dd, J = 13.9, 5.9 Hz, 1H), 3.05 (dd, J = 13.9, 6.9 Hz, 1H), 2.83 (dd, J = 14.9, 10.0 Hz, 1H); ^{13}C NMR (126 MHz, $CDCl_3$) δ 171.5, 170.4, 146.2, 136.3, 135.9, 133.4, 132.6, 131.7, 130.6, 129.3, 128.6, 127.1, 126.2, 125.5, 124.4, 122.1, 119.8, 118.4, 111.3, 108.8, 58.0, 53.4, 52.4, 37.9, 28.8; ESI HRMS (*m/z*): calcd for $C_{27}H_{26}N_4O_7S^+$ $[M+H]^+$: 551.1595, found: 551.1601.

4.6. Methyl N^{α}-(2-bromoethyl)- N^{α}-((2-nitrophenyl)sulfonyl)-L-tryptophyl-L-phenylalaninate **25**

To a cooled (0 °C) solution of **24** (4.38 g, 7.95 mmol), PPh_3 (3.13 g, 1.5 eq., 11.92 mmol) and 2-bromoethanol (0.56 mL, 1.0 eq., 7.95 mmol) in THF (100 mL) was added 40% solution of DEAD in toluene (4.34 mL, 1.2 eq., 9.34 mmol) dropwise. The reaction mixture is allowed to reach rt and stirred overnight. The resulting solution was evaporated and the residue was subjected to CC (automated, 80 g, SiO_2, *n*-hexane/AcOEt 3:1 to 1:1, then: automated, 40 g, RP-C18, water/MeOH gradient) to give **25** (4.01 g, 77%). White solid; ^{1}H NMR (300 MHz, $CDCl_3$) δ 7.77 (bs, 1H), 7.67–7.58 (m, 1H), 7.46–7.36 (m, 2H), 7.33–7.21 (m, 5H), 7.20–7.06 (m, 5H), 7.00 (ddd, J = 8.0, 6.6, 1.5 Hz, 1H), 6.96 (d, J = 2.3 Hz, 1H), 6.91 (d, J = 7.7 Hz, 1H), 4.68 (ddd, J = 9.2, 7.6, 4.8 Hz, 1H), 4.54 (dd, J = 8.2, 6.9 Hz, 1H), 3.94–3.78 (m, 1H), 3.78–3.61 (m, 4H), 3.35 (dd, J = 15.0, 6.8 Hz, 1H), 3.24–2.98 (m, 3H), 2.96–2.79 (m, 2H); ^{13}C NMR (75 MHz, $CDCl_3$) δ 172.0, 170.3, 147.5, 136.4, 136.2, 133.8, 132.4, 131.8, 131.3, 129.7, 129.4, 127.9, 127.2, 124.4, 124.3, 122.6, 120.2, 118.8, 111.7, 109.9, 59.7, 54.7, 52.9, 46.7, 38.2, 28.9, 24.7; LC-MS (*m/z*): 657 and 659 $[M+H]^+$.

4.7. Methyl (S)-2-((S)-3-((1H-indol-3-yl)methyl)-4-((2-nitrophenyl) sulfonyl)-2-oxopiperazin-1-yl)-3-phenylpropanoate **28**

To a solution of **25** (4.01 g, 6.10 mmol) in dry THF (150 mL) was added DBU (1.09 mL, 1.2 eq., 7.32 mmol) dropwise. The mixture was stirred overnight and concentrated *in vacuo*. The residue was partitioned between AcOEt (100 mL) and 1 M aqueous solution of HCl (50 mL). The mixture was shaken in a separatory funnel and the layers were separated. The aqueous phase was extracted with AcOEt (30 mL) and the combined organic extracts were washed with water (50 mL), saturated solution of NaCl (50 mL), dried over anhydrous Na_2SO_4, filtered and evaporated *in vacuo*. The residue was subjected to CC (automated, 80 g, SiO_2, *n*-hexane/AcOEt 1:1 to 0:1) to give **28** (3.51 g, 87%). Yellow solid; ^{1}H NMR (500 MHz, $CDCl_3$) δ 7.71 (bs, 1H), 7.49 (dq, J = 7.9, 0.9 Hz, 1H), 7.43 (dd, J = 7.8, 1.5 Hz, 1H), 7.40–7.33 (m, 2H), 7.31–7.25 (m, 2H), 7.24–7.20 (m, 1H), 7.19–7.15 (m, 2H), 7.08 (ddd, J = 5.4, 2.9, 1.2 Hz, 3H), 7.07–7.00 (m, 2H), 6.70 (d, J = 2.3 Hz, 1H), 5.19 (dd, J = 10.7, 5.6 Hz, 1H), 4.70 (ddd, J = 9.1, 4.0, 1.5 Hz, 1H), 3.92–3.84 (m, 1H), 3.71 (s, 3H), 3.34 (dd, J = 14.5, 5.6 Hz, 1H), 3.30–3.14 (m, 3H), 3.10–2.98 (m, 2H), 2.90 (dd, J = 15.1, 9.1 Hz, 1H); ^{13}C NMR (126 MHz, $CDCl_3$) δ 170.21, 167.29, 146.60, 136.52, 135.76, 133.09, 132.78, 131.55, 130.16, 128.96, 128.76, 126.95, 126.90, 123.88, 123.63, 121.92, 119.66, 118.75, 111.06, 110.33, 77.28, 77.03, 76.78, 59.88, 58.48, 52.47, 45.14, 39.68, 34.04, 27.79; ESI HRMS (*m/z*): calcd for $C_{29}H_{29}N_4O_7S^+$ $[M+H]^+$: 577.1752, found: 577.1758.

4.8. Methyl (S)-2-((S)-3-((1H-indol-3-yl)methyl)-2-oxopiperazin-1-yl)-3-phenylpropanoate **4**

A mixture of PhSH (0.78 mL, 7.61 mmol), Cs_2CO_3 (2.48 g, 1.0eq, 7.61 mmol) and acetonitrile (50 mL) was stirred for 1 h, followed by addition of **28** (2.20 g, 0.5 eq., 3.81 mmol). The stirring was continued overnight and the mixture was loaded on a short column (15 g of SiO_2, conditioned with *n*-hexanes). The column was eluted with *n*-hexanes until the eluate was colorless and no more non-polar byproducts were detected by TLC (AcOEt). SiO_2 was then dried, loaded on a column and the compound was purified by CC (automated, 40 g, SiO_2, AcOEt/MeOH/TEA 99:0:1 to AcOEt 96:4:1) to give **4** (0.97 g, 65%). Beige solid; Purity: 95.8% (LC-MS); ^{1}H NMR (500 MHz, $CDCl_3$) δ 8.19 (bs, 1H), 7.66 (dq, J = 7.9, 0.9 Hz, 1H), 7.37–7.29 (m, 3H), 7.29–7.22 (m, 3H), 7.19 (ddd, J = 8.2, 7.0, 1.2 Hz, 1H), 7.11 (ddd, J = 8.0, 7.0, 1.1 Hz, 1H), 6.87 (d, J = 2.4 Hz, 1H), 5.17 (dd, J = 10.9, 5.3 Hz, 1H), 3.80–3.69 (m, 4H), 3.45 (ddd, J = 14.5, 3.6, 1.0 Hz, 1H), 3.39 (dd, J = 14.5, 5.3 Hz, 1H), 3.26 (td, J = 10.7, 4.3 Hz, 1H), 3.12 (dd, J = 14.5, 10.9 Hz, 1H), 2.95 (dt, J = 11.0, 3.6 Hz, 1H), 2.93–2.87 (m, 2H), 2.76 (ddd, J = 12.6, 10.5, 3.9 Hz, 1H); ^{13}C NMR (126 MHz, $CDCl_3$) δ 171.1, 170.4, 137.2, 136.2, 129.0, 128.6, 127.5, 126.7, 123.1, 122.1, 119.4, 119.0, 111.7, 111.1, 59.8, 58.5, 52.3, 46.7, 41.9, 34.2, 27.6; ESI HRMS (*m/z*): calcd for $C_{23}H_{26}N_3O_3^+$ $[M+H]^+$: 392.1969, found: 392.1968.

4.9. Methyl ((4-nitrophenyl)sulfonyl)-L-tryptophyl-L-tryptophanate **24**

A solution of **22** (10.00 g, 25.68 mmol) in DMF (200 mL) is cooled (0 °C), followed by the addition of EDC (5.91 g, 1.2.eq., 30.82 mmol), HOBt (5.20 g, 1.5 eq., 38.52 mmol), L-H-Trp-OMe x HCl (6.54 g, 1.0 eq., 25.68 mmol) and DIPEA (9.96 mL, 3.0 eq., 77.04 mmol. The mixture was allowed to reach rt and stirred overnight. AcOEt (250 mL) and water (400 mL) were added and the mixture was shaken in a separatory funnel. The layers were separated and the aqueous phase was extracted with EA (2 × 50 mL). The combined organic extracts were washed with 1 M aqueous solution of citric acid (100 mL), water (100 mL), saturated aqueous solution of $NaHCO_3$ (75 mL), water (100 mL) and saturated aqueous solution of NH_4Cl (5 × 75 mL), dried over anhydrous Na_2SO_4, filtered and evaporated *in vacuo*. The residue was subjected to CC (manual, SiO_2, *n*-hexane/AcOEt 3:1 to 1:2) to give **24** (3.91 g, 26%). Yellow solid; ^{1}H NMR (300 MHz, $CDCl_3$) δ 8.06 (bs, 1H), 7.81 (bs, 1H), 7.75 (dd, J = 7.7, 1.5 Hz, 1H), 7.50 (d, J = 7.8 Hz, 1H), 7.46 (dd, J = 7.8, 1.6 Hz, 1H), 7.42–7.27 (m, 3H), 7.25–7.17 (m, 2H), 7.17–7.09 (m, 2H), 7.08–6.99 (m, 2H), 6.92–6.79 (m, 3H), 5.86 (d, J = 5.1 Hz, 1H), 4.88 (q, J = 6.1 Hz, 1H), 4.13 (dt, J = 9.8, 5.1 Hz, 1H), 3.68 (s, 3H), 3.38–3.16 (m, 3H), 2.73 (dd, J = 14.9, 9.4 Hz, 1H); ^{13}C NMR (75 MHz, $CDCl_3$) δ 171.8, 170.2, 146.2, 136.2, 136.1, 133.4, 132.6, 131.8, 130.6, 127.6, 126.3, 125.4, 123.1, 122.22, 122.16, 119.8, 119.6, 118.7, 118.5, 111.4, 111.2, 109.8, 109.0, 57.8, 52.9, 52.5, 28.4, 27.5; ESI HRMS (*m/z*): calcd for $C_{29}H_{28}N_5O_7S^+$ $[M+H]^+$: 590.1704, found: 590.1706.

4.10. Methyl N^{α}-(2-bromoethyl)- N^{α}-((2-nitrophenyl)sulfonyl)-L-tryptophyl-L-tryptophanate **26**

To a cooled (0 °C) solution of **24** (3.90 g, 6.61 mmol), PPh_3 (2.60 g, 1.5 eq., 9.92 mmol) and 2-bromoethanol (0.47 mL, 1.0 eq., 6.61 mmol) in THF (75 mL) was added 40% solution of DEAD in toluene (3.61 mL, 1.2 eq., 7.94 mmol) dropwise. The reaction mixture is allowed to reach rt and stirred overnight. The resulting solution was evaporated and the residue was subjected to CC (automated, 80 g, SiO_2, *n*-hexane/AcOEt 3:1 to 1:1, then: automated, 40 g, RP-C18, water/MeOH gradient) to give **26** (2.94 g, 64%). Yellow solid; ^{1}H NMR (500 MHz, $CDCl_3$) δ 8.07 (d, J = 2.3 Hz, 1H), 7.85 (d, J = 2.3 Hz, 1H), 7.55–7.48 (m, 2H), 7.37–7.28 (m, 2H), 7.28–7.23 (m, 2H), 7.20 (ddd, J = 8.2, 7.1, 1.2 Hz, 1H), 7.16–7.05 (m, 4H), 7.00 (ddd, J = 8.0, 6.6, 1.5 Hz, 1H), 6.93 (d, J = 2.4 Hz, 1H), 6.88 (d, J = 2.4 Hz, 1H), 6.81 (d, J = 6.9 Hz, 1H), 4.70 (ddd, J = 8.4, 6.9, 4.7 Hz, 1H), 4.57 (dd, J = 8.0, 7.1 Hz, 1H), 3.86 (ddd, J = 15.2, 11.4, 5.7 Hz, 1H), 3.76–3.65 (m, 4H), 3.30 (ddt, J = 14.9, 5.9, 1.1 Hz, 2H), 3.18–3.08 (m, 2H), 3.05 (dd, J = 15.1, 8.0 Hz, 1H), 2.88 (ddd, J = 11.1, 9.4, 5.8 Hz, 1H); ^{13}C NMR (126 MHz, $CDCl_3$) δ 172.0, 169.7, 147.0, 136.3, 135.9, 133.3, 131.7, 131.3, 130.6, 126.8, 126.6, 123.84, 123.78, 122.4, 122.0, 119.74, 119.66, 118.4, 118.3, 111.5, 111.2, 109.2, 109.2, 59.2, 52.8, 52.5, 46.4, 28.6, 27.5, 24.6; ESI HRMS (*m/z*): calcd for $C_{31}H_{31}N_5O_7SBr^+$ $[M+H]^+$: 696.11221 and 698.11016, found: 696.1122 and 698.1098.

4.11. Methyl (S)-2-((S)-3-((1H-indol-3-yl)methyl)-4-((2-nitrophenyl)sulfonyl)-2-oxopiperazin-1-yl)-3-(1H-indol-3-yl)propanoate **29**

To a solution of **26** (2.27 g, 3.26 mmol) in dry THF (60 mL) was added DBU (0.49 mL, 1.0 eq., 3.26 mmol) dropwise. The mixture was stirred overnight and concentrated *in vacuo*. The residue was partitioned between AcOEt (75 mL) and 1 M aqueous solution of HCl (30 mL). The mixture was shaken in a separatory funnel and the layers were separated. The aqueous phase was extracted with AcOEt (15 mL) and the combined organic extracts were washed with water (35 mL), saturated solution of NaCl (40 mL), dried over anhydrous Na_2SO_4, filtered and evaporated *in vacuo*. The residue was subjected to CC (automated, 40 g, SiO_2, *n*-hexane/AcOEt 3:1 to 0:1) to give **29** (1.69 g, 84%). Yellow solid; ^{1}H NMR (500 MHz, $CDCl_3$) δ 7.96 (d, J = 2.5 Hz, 1H), 7.71 (d, J = 2.2 Hz, 1H), 7.54–7.48 (m, 2H), 7.46 (dd, J = 8.0, 1.3 Hz, 1H), 7.45–7.42 (m, 1H), 7.39 (ddd, J = 7.9, 7.4, 1.3 Hz, 1H), 7.32 (dt, J = 8.1, 0.9 Hz, 1H), 7.19 (ddd, J = 8.2, 7.1, 1.2 Hz, 1H), 7.17–7.09 (m, 4H), 7.02 (ddd, J = 8.0, 6.5, 1.5 Hz, 1H), 6.76 (d, J = 2.4 Hz, 1H), 6.60 (d, J = 2.4 Hz, 1H), 5.23 (dd, J = 11.3, 4.8 Hz, 1H), 4.73 (ddd, J = 7.9, 4.3, 1.4 Hz, 1H), 3.73–3.64 (m, 4H), 3.40 (ddd, J = 15.7, 4.9, 1.2 Hz, 1H), 3.23 (dtd, J = 15.7, 4.5, 0.8 Hz, 2H), 3.16–3.06 (m, 2H), 2.96 (ddd, J = 14.8, 11.4, 3.6 Hz, 1H), 2.88 (ddd, J = 11.9, 3.6, 2.0 Hz, 1H); ^{13}C NMR (126 MHz, $CDCl_3$) δ 170.7, 167.5, 146.8, 136.0, 135.8, 133.01, 132.97, 131.7, 130.2, 127.1, 127.0, 124.0, 123.9, 123.0, 122.2, 121.8, 119.7, 119.6, 119.1, 118.2, 111.4, 111.0, 110.1, 110.0, 59.8, 57.6, 52.5, 44.5, 40.1, 28.0, 23.6; ESI HRMS (*m/z*): calcd for $C_{31}H_{30}N_5O_7S^+$ $[M+H]^+$: 616.1860, found: 616.1864.

4.12. Methyl (S)-2-((S)-3-((1H-indol-3-yl)methyl)-2-oxopiperazin-1-yl)-3-(1H-indol-3-yl)propanoate **5**

A mixture of PhSH (0.50 mL, 4.87 mmol), Cs_2CO_3 (1.59 g, 1.0eq, 4.87 mmol) and acetonitrile (35 mL) was stirred for 1 h, followed by addition of **29** (1.50 g, 0.5 eq., 3.81 mmol). The stirring was continued overnight and the mixture was loaded on a short column (10 g of SiO_2, conditioned with *n*-hexanes). The column was eluted with *n*-hexanes until the eluate was colorless and no more non-polar byproducts were detected by TLC (AcOEt). SiO_2 was then dried, loaded on a column and the compound was purified by CC (automated, 40 g, SiO_2, AcOEt/MeOH/TEA 99:0:1 to 97:2:1) to give **5** (0.93 g, 86%). White solid; Purity: 95.4% (LC-MS); ^{1}H NMR (400 MHz, $CDCl_3$) δ 8.05–7.98 (m, 2H), 7.69 (dq, J = 7.9, 0.7 Hz, 1H), 7.57 (dq, J = 7.9, 0.7 Hz, 1H), 7.37–7.30 (m, 2H), 7.23–7.17 (m, 2H), 7.16–7.08 (m, 2H), 6.75 (d, J = 2.4 Hz, 1H), 6.72 (d, J = 2.4 Hz, 1H), 5.44 (dd, J = 11.5, 4.7 Hz, 1H), 3.81–3.73 (m, 4H), 3.41 (ddd, J = 15.7, 4.7, 1.2 Hz, 1H), 3.34 (ddd, J = 14.5, 4.0, 0.9 Hz, 1H), 3.28–3.13 (m, 2H), 3.11 (dd, J = 10.8, 4.6 Hz, 1H), 3.04 (ddd, J = 11.3, 4.0, 2.4 Hz, 1H), 2.87 (ddd, J = 12.9, 4.5, 2.3 Hz, 1H), 2.80 (ddd, J = 12.8, 10.5, 4.1 Hz, 1H); ^{13}C NMR (101 MHz, $CDCl_3$) δ 171.6, 170.8, 136.2, 136.0, 127.8, 127.3, 123.5, 122.5, 122.1, 122.0, 119.52, 119.49, 119.4, 118.5, 111.4, 111.2, 111.0, 110.9, 59.9, 56.9, 52.4, 45.7, 42.0, 27.3, 23.8; ESI HRMS (*m/z*): calcd for $C_{25}H_{27}N_4O_3^+$ $[M+H]^+$: 431.2077, found: 431.2078.

4.13. (S)-2-((S)-3-((1H-indol-3-yl)methyl)-2-oxopiperazin-1-yl)-3-(1H-indol-3-yl)propanamide **6**

A solution of **5** (115 mg, 267 μmol) in 7 N HN_3 MeOH (5 mL) was refluxed for 24 h in a pressure tube. The mixture was then evaporated

and purified by CC (automated, 4 g, SiO_2, AcOEt/MeOH/TEA 99:0:1 to 94:5:1) to give **6** (81 mg, 73%). White solid; Purity: >95% (^{1}H NMR); ^{1}H NMR (400 MHz, DMSO) δ 10.80 (bs, 1H), 10.77 (bs, 1H), 7.61 (d, J = 7.6 Hz, 1H), 7.50 (d, J = 7.6 Hz, 1H), 7.39–7.29 (m, 4H), 7.15–6.94 (m, 7H), 5.37–5.29 (m, 1H), 3.60–3.52 (m, 1H), 3.23 (d, J = 13.7 Hz, 4H), 3.01 (dd, J = 14.7, 10.5 Hz, 1H), 2.86 (d, J = 12.6 Hz, 1H), 2.78–2.61 (m, 2H), 2.10 (bs, 1H); ^{13}C NMR (101 MHz, DMSO) δ 172.5, 170.4, 136.6, 136.5, 128.5, 127.8, 127.7, 126.9, 124.0, 123.2, 121.4, 121.3, 118.80, 118.77, 118.72, 118.68, 111.80, 111.76, 111.5, 110.8, 63.4, 60.1, 56.0, 44.44, 41.61, 28.33, 23.95; ESI HRMS (*m/z*): calcd for $C_{24}H_{26}N_5O_2^+$ $[M+H]^+$: 416.2081, found: 416.2079.

4.14. Methyl (S)-2-((S)-3-((1H-indol-3-yl)methyl)-4-acetyl-2-oxopiperazin-1-yl)-3-(1H-indol-3-yl)propanoate **7**

A solution of **6** (62 mg, 144 μmol) and DMAP (1 mg, 0.05 eq., 7 μmol) in dry DCM (1 mL) was cooled (0 °C). DIPEA (38 μL, 1.5 eq., 216 μmol) and Ac_2O (16 μL, 1.2 eq., 173 μmol) were added and the resulting mixture was allowed to reach rt and stirred overnight. The solution was evaporated *in vacuo* and the residue was subjected to CC (manual, SiO_2, *n*-hexane/AcOEt 4:1 to 0:1), to give **7** (62 mg, 91%). White solid; Purity: 98.0% (LC-MS); ^{1}H NMR (400 MHz, $CDCl_3$, rotamers in a 1:1 ratio) δ 8.38 (bs, 1H), 8.33–8.26 (m, 2H), 7.87 (bs, 1H), 7.60–7.53 (m, 2H), 7.52–7.43 (m, 2H), 7.37 (d, J = 8.1 Hz, 1H), 7.35–7.29 (m, 2H), 7.25–7.21 (m, 2H), 7.21–7.02 (m, 7H), 6.88 (d, J = 2.1 Hz, 1H), 6.75 (d, J = 1.9 Hz, 1H), 6.63 (d, J = 1.9 Hz, 1H), 6.33 (d, J = 2.2 Hz, 1H), 5.58 (dd, J = 11.3, 4.7 Hz, 1H), 5.40 (dd, J = 10.8, 5.2 Hz, 1H), 5.18 (t, J = 4.3 Hz, 1H), 4.47 (dd, J = 8.5, 3.1 Hz, 1H), 4.35 (d, J = 13.6 Hz, 1H), 3.78 (s, 3H), 3.76 (s, 3H), 3.50–3.26 (m, 5H), 3.26–2.99 (m, 6H), 2.87 (dd, J = 14.6, 8.8 Hz, 1H), 2.71 (dt, J = 11.8, 3.5 Hz, 1H), 2.58 (ddd, J = 14.8, 11.1, 3.9 Hz, 1H), 2.33 (ddd, J = 13.2, 9.7, 3.3 Hz, 1H), 1.95 (s, 3H), 1.40 (s, 3H); ^{13}C NMR (101 MHz, $CDCl_3$, rotamers in a 1:1 ratio) δ 171.2, 170.7, 169.8, 169.2, 169.0, 168.0, 136.04, 136.00, 135.98, 135.8, 128.1, 127.33, 127.28, 127.1, 123.6, 123.4, 122.8, 122.4, 122.3, 122.2, 122.1, 121.7, 119.9, 119.61, 119.58, 119.4, 118.9, 118.44, 118.38, 118.29, 111.4, 111.33, 111.29, 111.0, 110.9, 110.4, 110.10, 110.07, 60.4, 57.5, 57.4, 56.4, 52.53, 52.51, 43.4, 42.7, 42.6, 35.5, 27.7, 25.9, 23.7, 21.7, 20.2; LC-MS (*m/z*): 473 $[M+H]^+$.

4.15. Methyl N^{α}-(3-bromopropyl)- N^{α}-((2-nitrophenyl)sulfonyl)-L-tryptophyl-L-tryptophanate

To a cooled (0 °C) solution of **24** (3.90 g, 6.61 mmol), PPh_3 (2.60 g, 1.5 eq., 9.92 mmol) and 2-bromoethanol (0.60 mL, 1.0 eq., 6.61 mmol) in THF (75 mL) was added 40% solution of DEAD in toluene (3.61 mL, 1.2 eq., 7.94 mmol) dropwise. The reaction mixture is allowed to reach rt and stirred overnight. The resulting solution was evaporated and the residue was subjected to CC (manual, SiO_2, *n*-hexane/AcOEt 3:1 to 1:1, then: automated, 40 g, RP-C18, water/MeOH gradient) to give **27** (3.68 g, 78%). Yellow solid; ^{1}H NMR (300 MHz, $CDCl_3$) δ 8.07 (bs, 1H), 7.73 (bs, 1H), 7.57 (d, J = 7.8 Hz, 1H), 7.51 (d, J = 8.0 Hz, 1H), 7.36 (d, J = 8.1 Hz, 1H), 7.32–7.28 (m, 2H), 7.27–7.23 (m, 1H), 7.23–7.16 (m, 1H), 7.15–7.08 (m, 3H), 7.07–6.96 (m, 4H), 6.90 (d, J = 2.2 Hz, 1H), 4.70 (ddd, J = 9.3, 6.6, 4.4 Hz, 1H), 4.58 (dd, J = 8.5, 6.5 Hz, 1H), 3.74 (s, 3H), 3.62 (ddd, J = 16.0, 10.6, 5.1 Hz, 1H), 3.53–3.28 (m, 3H), 3.17–2.96 (m, 2H), 2.86 (t, J = 6.0 Hz, 2H), 1.74–1.53 (m, 1H), 1.35–1.15 (m, 1H); ^{13}C NMR (75 MHz, $CDCl_3$) δ 172.4, 170.3, 146.9, 136.5, 136.0, 133.2, 132.1, 131.3, 130.6, 127.0, 126.9, 124.3, 124.1, 123.8, 122.5, 122.0, 119.8, 119.7, 118.7, 118.5, 111.7, 111.4, 109.6, 109.5, 59.2, 53.1, 52.7, 44.5, 31.7, 30.8, 27.7, 23.9; ESI HRMS (*m/z*): calcd for $C_{32}H_{33}N_5O_7SBr^+$ $[M+H]^+$: 710.1279 and 712.1258, found: 710.1277 and 712.1253.

4.16. Methyl (S)-2-((S)-3-((1H-indol-3-yl)methyl)-4-((2-nitrophenyl)sulfonyl)-2-oxo-1,4-diazepan-1-yl)-3-(1H-indol-3-yl)propanoate **30**

To a solution of **27** (2.86 g, 4.02 mmol) in acetonitrile (60 mL) was added Cs_2CO_3 (1.57 g, 1.2 eq., 4.83 mmol) and KI (0.17 g, 0.1 eq., 0.40 mmol). The mixture was stirred at 50 °C for 6 h and at rt overnight and concentrated *in vacuo*. The residue was partitioned between AcOEt (75 mL) and water (30 mL). The mixture was shaken in a separatory funnel and the layers were separated. The aqueous phase was extracted with AcOEt (15 mL) and the combined organic extracts were washed with water (35 mL), saturated solution of NaCl (40 mL), dried over anhydrous Na_2SO_4, filtered and evaporated *in vacuo*. The residue was subjected to CC (automated, 40 g, SiO_2, *n*-hexane/AcOEt 3:1 to 0:1) to give **30** (0.74 g, 29%). Yellow solid; ^{1}H NMR (500 MHz, $CDCl_3$) δ 8.06 (bs, 1H), 7.83 (s, 1H), 7.59 (d, J = 7.8 Hz, 1H), 7.50 (d, J = 7.9 Hz, 1H), 7.41 (d, J = 7.9 Hz, 1H), 7.33 (dt, J = 8.1, 0.9 Hz, 1H), 7.30 (dd, J = 8.0, 1.3 Hz, 1H), 7.22–7.15 (m, 2H), 7.13–7.05 (m, 4H), 6.97 (ddd, J = 7.9, 6.6, 1.4 Hz, 1H), 6.90 (t, J = 7.6 Hz, 1H), 6.76 (d, J = 2.4 Hz, 1H), 4.92 (dd, J = 10.7, 4.7 Hz, 1H), 4.79 (d, J = 9.6 Hz, 1H), 3.89 (bs, 1H), 3.76 (s, 3H), 3.52 (ddd, J = 15.4, 4.9, 1.1 Hz, 1H), 3.41 (dd, J = 15.4, 10.7 Hz, 1H), 3.36–3.20 (m, 2H), 3.17 (d, J = 14.8 Hz, 1H), 3.04 (dd, J = 15.1, 10.3 Hz, 1H), 1.59 (bs, 2H); ^{13}C NMR (75 MHz, $CDCl_3$) δ 171.8, 171.4, 146.3, 136.4, 136.1, 132.9, 131.5, 130.9, 127.3, 126.7, 124.2, 123.9, 123.7, 122.1, 122.0, 119.8, 119.6, 118.8, 118.4, 111.6, 111.4, 111.0, 109.6, 63.1, 63.0, 52.6, 47.5, 43.3 (bs), 29.2, 24.8, 24.7; ESI HRMS (*m/z*): calcd for $C_{32}H_{32}N_5O_7S^+$ $[M+H]^+$: 630.2017, found: 630.2020.

4.17. Methyl (S)-2-((S)-3-((1H-indol-3-yl)methyl)-2-oxo-1,4-diazepan-1-yl)-3-(1H-indol-3-yl)propanoate **8**

A mixture of PhSH (0.24 mL, 2.38 mmol), Cs_2CO_3 (0.78 g, 1.0eq, 2.38 mmol) and acetonitrile (30 mL) was stirred for 1 h, followed by addition of **30** (0.75 g, 0.5 eq., 1.19 mmol). The stirring was continued overnight and the mixture was loaded on a short column (8 g of SiO_2, conditioned with *n*-hexanes). The column was eluted with *n*-hexanes until the eluate was colorless and no more non-polar byproducts were detected by TLC (AcOEt). SiO_2 was then dried, loaded on a column and the compound was purified by CC (automated, 24 g, SiO_2, AcOEt/MeOH/TEA 99:0:1 to AcOEt 97:2:1) to give **8** (0.53 g, 78%). White solid; Purity: 98.0% (LC-MS); ^{1}H NMR (500 MHz, $CDCl_3$) δ 8.31 (d, J = 2.2 Hz, 1H), 8.03 (d, J = 2.3 Hz, 1H), 7.63 (dq, J = 7.9, 0.8 Hz, 1H), 7.53 (dq, J = 7.9, 0.8 Hz, 1H), 7.37 (dt, J = 8.1, 0.9 Hz, 1H), 7.28 (dt, J = 8.2, 0.9 Hz, 1H), 7.22 (ddd, J = 8.2, 7.1, 1.2 Hz, 1H), 7.17–7.11 (m, 2H), 7.06–6.99 (m, 2H), 6.74 (d, J = 2.3 Hz, 1H), 5.11 (dd, J = 10.0, 5.4 Hz, 1H), 3.74 (s, 3H), 3.67 (dd, J = 8.5, 5.7 Hz, 1H), 3.49–3.37 (m, 2H), 3.39–3.26 (m, 2H), 3.11 (ddd, J = 15.8, 6.2, 2.2 Hz, 1H), 3.07–2.98 (m, 2H), 2.57 (ddd, J = 13.1, 11.3, 3.6 Hz, 1H), 1.55–1.40 (m, 2H); ^{13}C NMR (75 MHz, $CDCl_3$) δ 171.9171.4, 146.3, 136.4, 136.1,9 132., 131.5, 130.9, 127.3, 126.7, 124.2, 123.9, 123.7, 122.1, 122.0, 119.8, 119.6, 118.8, 118.4, 111.6, 111.4, 111.0, 109.6, 63.1, 63.0, 52.6, 47.5, 43.3, 29.2, 24.9, 24.7; ESI HRMS (*m/z*): calcd for $C_{26}H_{29}N_4O_3^+$ $[M+H]^+$: 445.2234, found: 445.2233.

4.18. Methyl (tert-Butoxycarbonyl)-L-tryptophyl-L-phenylalaninate **31**

A solution of L-Boc-Trp-OH (3.50 g, 11.5 mmol) in DMF (50 mL) was cooled (0 °C), followed by the addition of DIPEA (6.01 mL, 3.0 eq., 34.5 mmol) and TBTU (5.54 g, 1.5 eq., 17.2 mmol). After 30 min, L-H-Phe-OMe x HCl (3.72 g, 1.5 eq., 17.2 mmol) was added and the mixture was allowed to reach rt and stirred overnight. AcOEt (100 mL) and water (100 mL) were added and the mixture was shaken in a separatory funnel. The layers were separated and the aqueous phase was extracted with EA (50 mL). The combined organic extracts were washed with 1 M aqueous solution of citric acid (40 mL), water (40 mL), saturated aqueous solution of $NaHCO_3$ (40 mL), water (40 mL) and saturated aqueous solution of NH_4Cl (3 × 40 mL), dried over anhydrous Na_2SO_4, filtered and

evaporated *in vacuo*. The residue was subjected to CC (manual, SiO_2, *n*-hexane/AcOEt 3:1 to 1:2) to give **31** (4.19 g, 78%). White solid; ^{1}H NMR (300 MHz, $CDCl_3$) δ 8.01 (bs, 1H), 7.66 (d, J = 7.7 Hz, 1H), 7.36 (d, J = 8.2 Hz, 1H), 7.24–7.08 (m, 4H), 7.02 (s, 1H), 6.87–6.75 (m, 2H), 6.18 (d, J = 7.5 Hz, 1H), 5.09 (bs, 1H), 4.79–4.67 (m, 1H), 4.42 (bs, 1H), 3.62 (s, 3H), 3.31 (bs, 1H), 3.13 (dd, J = 14.6, 7.2 Hz, 1H), 2.94 (d, J = 5.8 Hz, 2H), 1.42 (s, 9H); ^{13}C NMR (75 MHz, $CDCl_3$) δ 171.3, 171.2, 136.2, 135.6, 129.2, 128.5, 127.5 (bs), 127.0, 123.3, 122.4, 119.9, 119.0, 111.2, 110.8 (bs), 55.2 (bs), 53.2, 52.2, 37.9, 28.3; ESI HRMS (*m/z*): calcd for $C_{26}H_{32}N_3O_5^+$ $[M+H]^+$: 446.2336, found: 446.2338.

4.19. Methyl (2-bromoacetyl)-L-tryptophyl-L-phenylalaninate **32**

A mixture of **31** (2.67, 7.30 mmol) and 4 M solution of HCl in 1,4-dioxane (40 mL) was stirred at rt for 3 h. Argon was bubbled through the mixture followed by evaporation *in vacuo*. The residue was dissolved in dry DCM (40 mL) and solution was cooled (0 °C). DMAP (49.0 mg, 0.05 eq., 401 μmol) and DIPEA (2.92 mL, 2.3 eq., 16.78 mmol) were added followed by a slow addition of bromoacetyl chloride (0.67 mL, 1.1 eq., 8.02 mmol). The mixture was allowed to reach rt and stirred overnight. 1 M aqueous solution of citric acid (20 mL) was added and the mixture was shaken in a separatory funnel. The layers were separated and the aqueous phase was washed with DCM (20 mL). The combined organic extract was washed with water (20 mL), saturated aqueous solution of $NaHCO_3$ (20 mL), water (20 mL), saturated aqueous solution of NaCl (20 mL), dried over anhydrous Na_2SO_4, filtered and evaporated *in vacuo*. The residue was subjected to CC (automated, 80 g, SiO_2, *n*-hexane/AcOEt 3:1 to 1:2) to give **32** (1.86 g, 52%). White solid; ^{1}H NMR (500 MHz, DMSO) δ 10.83 (d, J = 2.4 Hz, 1H), 8.62 (d, J = 7.6 Hz, 1H), 8.30 (d, J = 8.2 Hz, 1H), 7.32 (dt, J = 8.1, 0.9 Hz, 1H), 7.29–7.24 (m, 2H), 7.23–7.18 (m, 3H), 7.09 (d, J = 2.4 Hz, 1H), 7.06 (ddd, J = 8.1, 6.9, 1.2 Hz, 1H), 6.98 (ddd, J = 7.9, 6.9, 1.1 Hz, 1H), 4.62 (td, J = 8.4, 5.2 Hz, 1H), 4.50 (ddd, J = 8.7, 7.6, 5.9 Hz, 1H), 4.03 (d, J = 3.9 Hz, 2H), 3.58 (s, 3H), 3.14–3.00 (m, 2H), 2.99–2.88 (m, 2H); ^{13}C NMR (126 MHz, DMSO) δ 171.7, 171.1, 165.4, 137.1, 136.0, 129.1, 128.3, 127.3, 126.6, 123.6, 120.9, 118.4, 118.2, 111.3, 109.5, 53.7, 53.2, 51.8, 42.5, 36.6, 27.8; ESI HRMS (*m/z*): calcd for $C_{23}H_{25}N_3O_4Br^+$ $[M+H]^+$: 486.1023 and 488.1002, found: 486.1020 and 488.0999.

4.20. Methyl (S)-2-((S)-3-((1H-indol-3-yl)methyl)-2,5-dioxopiperazin-1-yl)-3-phenylpropanoate **9**

A mixture of **32** (500 mg, 1.03 mmol), Cs_2CO_3 (335 mg, 1.0 eq., 1.03 mmol) and dry DMF (10 mL) was stirred at rt overnight. AcOEt (30 mL) and water (50 mL) were added and the mixture was shaken in a separatory funnel. The layers were separated and the aqueous phase was extracted with EA (20 mL). The combined organic extracts were washed water (20 mL), saturated aqueous solution of NH_4Cl (20 mL), dried over anhydrous Na_2SO_4, filtered and evaporated *in vacuo*. The residue was subjected to CC (manual, SiO_2, *n*-hexane/AcOEt 1:1 to 0:1) to give **9** (224 mg, 54%); White solid; Purity: >95% (^{1}H NMR); ^{1}H NMR (300 MHz, DMSO) δ 10.82 (bs, 1H), 8.61 (d, J = 7.6 Hz, 1H), 8.30 (d, J = 8.4 Hz, 1H), 7.58 (d, J = 7.8 Hz, 1H), 7.36–7.15 (m, 5H), 7.13–7.02 (m, 2H), 6.98 (t, J = 7.4 Hz, 1H), 4.62 (td, J = 8.3, 5.1 Hz, 1H), 4.50 (td, J = 8.1, 6.0 Hz, 1H), 4.03 (d, J = 1.5 Hz, 2H), 3.58 (s, 3H), 3.17–2.86 (m, 4H); ^{13}C NMR (75 MHz, DMSO) δ 172.2, 171.6, 165.9, 137.5, 136.5, 129.5, 128.7, 127.8, 127.04, 124.07, 121.3, 118.8, 118.7, 111.7, 110.0, 54.1, 53.7, 52.3, 43.0, 37.1, 28.3; ESI HRMS (*m/z*): calcd for $C_{23}H_{24}N_3O_4^+$ $[M+H]^+$: 406.1761, found: 406.1759.

4.21. (S)-2-((S)-3-((1H-indol-3-yl)methyl)-2,5-dioxopiperazin-1-yl)-3-phenylpropanamide **10**

A solution of **9** (75 mg, 185 μmol) in 7 N HN_3 MeOH (4 mL) was refluxed for 24 h in a pressure tube. The mixture was then evaporated and purified by CC (automated, 4 g, SiO_2, DCM/MeOH 99:1 to 90:10) to give **10** (60 mg, 83%). White solid; Purity: >95% (^{1}H NMR); ^{1}H NMR (500 MHz, MeOD) δ 7.59–7.56 (m, 1H), 7.37–7.35 (m, 1H), 7.26–7.21 (m, 2H), 7.20–7.15 (m, 1H), 7.11–7.06 (m, 4H), 6.96 (s, 1H), 5.00 (dd, J = 9.9, 6.0 Hz, 1H), 4.27 (t, J = 4.3 Hz, 1H), 3.84 (d, J = 17.2 Hz, 1H), 3.36–3.32 (m, 1H, partially overlapped with solvent signal), 3.01 (dd, J = 14.7, 4.1 Hz, 1H), 2.76–2.63 (m, 2H), 1.67 (dd, J = 13.3, 6.0 Hz, 1H); ^{13}C NMR (126 MHz, MeOD) δ 173.4, 168.6, 168.3, 137.9, 137.8, 130.2, 129.4, 128.7, 127.8, 125.9, 122.8, 120.3, 119.6, 112.6, 109.0, 57.8, 57.6, 46.7, 34.4, 31.3. LC-MS (*m/z*): 391 $[M+H]^+$.

4.22. tert-Butyl (S)-(1-hydroxy-3-(1H-indol-3-yl)propan-2-yl) carbamate **33**

To a stirred, cooled (0 °C) suspension of LAH (17.28 g, 3.1 eq., 455.37 mmol) in anhydrous THF (1000 mL) L-H-Trp-OH (30.00 g, 146.90 mmol) was added in small batches. Then solution was stirred at rt for 30 min before being slowly heated to reflux. After 48 h the reaction mixture was cooled (0 °C) and water (90 mL) was slowly added, followed by 15% aqueous solution of NaOH (90 mL) and water (270 mL). Vigorous stirring was maintained for 30 min and the granular inorganic precipitate formed was removed by suction filtration washed with AcOEt (400 mL). The filtrate was evaporated *in vacuo* and the residue was dissolved in AcOEt (300 mL), washed with saturated aqueous solution of NaCl (3 × 100mL), dried over anhydrous $MgSO_4$, filtered and evaporated *in vacuo*. A portion of obtained crude L-H-Trp-ol (10.00 g, 52.56 mmol) was dissolved in a mixture of THF (60 mL) and water (60 mL). $NaHCO_3$ (8.83 g, 2.0 eq.,105.12 mmol) was added and the mixture was cooled (0 °C). A solution of di-*tert*-butyl decarbonate (17.21 g, 1.5 eq., 78.85 mmol) in THF (60 mL) was added. After 15 min, the reaction mixture was brought to rt and stirred overnight. AcOEt (100 mL) was added and the layers were separated. The aqueous phase was extracted with AcOEt (2 × 50 mL). The combined organic phase was sequentially washed with water (75 mL), 1 M aqueous solution of citric acid (50 mL), water (50 mL), saturated aqueous solution of $NaHCO_3$ (50 mL), dried over anhydrous Na_2SO4, filtered and evaporated *in vacuo*. The obtained **33** (13.87 g, 91%) was pure enough for the subsequent reactions. Pale-yellow solid; ^{1}H NMR (400 MHz, DMSO) δ 10.74 (d, J = 2.4 Hz, 1H), 7.56 (d, J = 7.8 Hz, 1H), 7.31 (dt, J = 8.1, 0.9 Hz, 1H), 7.07 (d, J = 2.3 Hz, 1H), 7.04 (ddd, J = 8.1, 7.0, 1.2 Hz, 1H), 6.95 (ddd, J = 8.0, 7.0, 1.1 Hz, 1H), 6.51 (d, J = 8.3 Hz, 1H), 4.61 (t, J = 5.7 Hz, 1H), 3.64 (p, J = 6.6 Hz, 1H), 3.41–3.25 (m, 3H), 2.87 (dd, J = 14.5, 6.3 Hz, 1H), 2.70 (dd, J = 14.5, 7.3 Hz, 1H), 1.34 (s, 9H). LC-MS (*m/z*): 291 $[M+H]^+$, 235 $[M\text{-}t\text{Bu}+H]^+$, 191 $[M\text{-}COOt\text{Bu}+H]^+$.

4.23. tert-Butyl (S)-(1-(1H-indol-3-yl)-3-oxopropan-2-yl)carbamate **34**

To the cooled (0 °C) solution of **33** (6.00 g, 19.71 mmol) in DMSO (40 mL) was added TEA (8.24 mL, 3.0 eq., 59.14 mmol). A solution of $PySO_3$ (9.41 g, 3.0 eq., 59.14 mmol) in DMSO (40 mL) was added. The solution was warmed to rt and stirred for 10 min. The mixture was added to cooled saturated aqueous solution of NaCl (300 mL) and extracted with Et_2O (2 × 100 mL). The combined organic layer was washed with 1 M aqueous solution of citric acid (2 × 75 mL), water (2 × 75 mL), saturated aqueous solution of $NaHCO_3$ (2 × 75 mL), water (2 × 75 mL), saturated aqueous solution of NaCl (100 mL), dried over anhydrous Na_2SO_4, filtered and evaporated *in vacuo* (at rt). The crude product was dried under high vacuum for 1 h and used immediately in the subsequent reactions.

4.24. Methyl ((S)-2-((tert-butoxycarbonyl)amino)-3-(1H-indol-3-yl) propyl)-L-phenylalaninate **35**

A mixture of **34** (1.84 g, 6.07 mmol), L-H-Phe-OMe x HCl (1.31 g, 1.0 eq., 6.07 mmol), TEA (0.85 mL, 1.0 eq., 6.07 mmol) and dry THF (50 mL) was stirred at rt for 30 min. AcOH (0.35 mL, 1.0 eq., 6.07 mmol) and $NaBH(OAc)_3$ (1.93 g, 1.5 eq., 9.11 mmol) were added and the mixture

was stirred at rt overnight. AcOEt (100 mL) and 2 M aqueous solution of NaOH (40 mL) were added, and the mixture was stirred vigorously for 20 min. The layers were separated and the aqueous phase was extracted with AcOEt (30 mL). The combined organic extracts were washed with water (50 mL), saturated aqueous solution of NaCl (40 mL), dried over anhydrous Na_2SO_4, filtered and evaporated *in vacuo*. The residue was subjected to CC (manual, SiO_2, *n*-hexane/AcOEt 3:1 to 1:2) to give **35** (1.60 g, 58%). Beige solid; ^{1}H NMR (400 MHz, $CDCl_3$) δ 8.09 (bs, 1H), 7.58 (d, J = 7.9 Hz, 1H), 7.39–7.28 (m, 4H), 7.23–7.16 (m, 3H), 7.15–7.07 (m, 1H), 6.83 (d, J = 2.3 Hz, 1H), 4.83 (bs, 1H), 3.93 (bs, 1H), 3.66 (s, 3H), 3.47 (dd, J = 8.0, 5.9 Hz, 1H), 3.04–2.82 (m, 4H), 2.70 (dd, J = 12.1, 5.2 Hz, 1H), 2.44 (dd, J = 12.1, 5.7 Hz, 1H), 1.61 (bs, 1H)*, 1.46 (bs, 8H)*; ^{13}C NMR (101 MHz, $CDCl_3$) δ 174.9, 155.7, 137.5, 136.2, 129.2, 128.5, 127.9 (bs), 126.8, 122.6, 122.0, 119.4, 119.1 (bs), 112.0, 111.0, 78.8 (bs), 63.2, 51.7, 50.9 (bs), 50.0 (bs), 39.6, 28.4*, 27.9 (bs)*. Broadened, low intensity signals are observed in the carbon spectrum due to the dynamic processes. * - rotamers. ESI HRMS (*m/z*): calcd for $C_{26}H_{34}N_3O_4^+$ $[M+H]^+$: 452.2544, found: 425.2542.

4.25. Methyl N-((S)-2-((tert-butoxycarbonyl)amino)-3-(1H-indol-3-yl) propyl)-N-(2-ethoxy-2-oxoethyl)-L-phenylalaninate **37**

A solution of **35** (433 mg, 0.93 mmol), DIPEA (486 μL, 3.0 eq., 2.79 mmol) and ethyl bromoacetate (206 μL, 2.0 eq., 1.86 mmol) in ACN (10 mL) was stirred at 50° for 5 h. Another portion of DIPEA (486 μL, 3.0 eq., 2.79 mmol) and ethyl bromoacetate (206 μL, 2.0 eq., 1.86 mmol) was added and the stirring was continued overnight. The mixture was evaporated *in vacuo* and the residue was subjected to CC (automated, 12 g, SiO_2, petroleum ether/AcOEt 9:1 to 1:1) to give **37** (212 mg, 78%). Beige solid; ^{1}H NMR (400 MHz, $CDCl_3$) δ 8.09 (bs, 1H), 7.63 (d, J = 7.8 Hz, 1H), 7.37 (d, J = 8.0 Hz, 1H), 7.26–7.09 (m, 7H), 6.97 (d, J = 2.4 Hz, 1H), 5.12 (bs, 1H), 4.15 (qd, J = 7.1, 1.4 Hz, 2H), 3.91 (bs, 1H), 3.70–3.50 (m, 6H), 3.11–2.83 (m, 5H), 2.77 (dd, J = 13.7, 7.1 Hz, 1H), 1.45 (bs, 9H), 1.26 (t, J = 7.1 Hz, 3H); ^{13}C NMR (101 MHz, $CDCl_3$) δ 172.5, 171.9, 155.9, 137.8, 136.2, 129.2, 128.4, 127.9 (bs), 126.5, 122.5, 121.9, 119.4, 119.2 (bs), 112.3, 111.0, 78.9 (bs), 66.6, 60.68, 56.2 (bs), 52.6, 51.5, 50.1 (bs), 35.8 (bs), 28.4, 14.2. Broadened, low intensity signals are observed in the carbon spectrum due to the dynamic processes; ESI HRMS (*m/z*): calcd for $C_{30}H_{40}N_3O_6^+$ $[M+H]^+$: 538.2912, found: 538.2915.

4.26. Methyl (S)-2-((S)-3-((1H-indol-3-yl)methyl)-5-oxopiperazin-1-yl)-3-phenylpropanoate **11** and ethyl 2-((2S,5S)-5-((1H-indol-3-yl) methyl)-2-benzyl-3-oxopiperazin-1-yl)acetate **39**

A mixture of **37** (370 mg, 0.69 mmol) and 4 M solution of HCl in 1,4-dioxane (4 mL) was stirred at rt for 2 h. Argon was bubbled through the mixture followed by evaporation *in vacuo*. The residue was partitioned between AcOEt (5 mL) and saturated aqueous solution of $NaHCO_3$ (3 mL). The layers were separated and the aqueous phase was washed with AcOEt (2 mL). The combined organic fraction was washed with saturated aqueous solution of NaCl (2 mL), dried, filtered and evaporated *in vacuo*. The residue was subjected to CC (automated, 4 g, SiO_2, petroleum ether/AcOEt 9:1 to 1:5) to give **11** (100 mg, 37%) and **39** (61 mg, 22%). **11**: White solid; Purity: 95.1% (LC-MS); ^{1}H NMR (400 MHz, $CDCl_3$) δ 8.36 (bs, 1H), 7.54–7.47 (m, 1H), 7.39 (dt, J = 8.2, 1.0 Hz, 1H), 7.35–7.30 (m, 2H), 7.28–7.19 (m, 4H), 7.15 (ddd, J = 8.1, 7.0, 1.1 Hz, 1H), 6.93 (d, J = 2.4 Hz, 1H), 5.90 (bs, 1H), 3.76–3.64 (m, 4H), 3.57 (t, J = 7.7 Hz, 1H), 3.48 (d, J = 16.5 Hz, 1H), 3.40 (d, J = 17.6 Hz, 1H), 3.21 (dd, J = 12.3, 3.8 Hz, 1H), 3.14 (dd, J = 13.8, 7.7 Hz, 1H), 3.04–2.94 (m, 2H), 2.76 (dd, J = 14.2, 9.0 Hz, 1H), 2.57 (dd, J = 12.0, 7.2 Hz, 1H); ^{13}C NMR (101 MHz, $CDCl_3$) δ 171.51 169.0, 137.6, 136.5, 129.1, 128.5, 127.0, 126.7, 123.0, 122.4, 119.7, 118.5, 111.5, 110.6, 67.4, 53.8, 52.1, 51.4, 50.8, 35.5, 30.3; ESI HRMS (*m/z*): calcd for $C_{23}H_{26}N_3O_3^+$ $[M+H]^+$: 392.1969, found: 392.1968.**39**: White solid ^{1}H NMR (400 MHz, $CDCl_3$) δ 8.20 (bs, 1H), 7.44–7.31 (m, 6H), 7.28–7.23 (m, 1H), 7.20 (ddd, J = 8.2, 7.0, 1.2 Hz, 1H), 7.11 (ddd, J = 8.0, 7.0, 1.0 Hz, 1H), 6.75 (d, J = 2.4 Hz, 1H), 5.94 (d, J = 3.3 Hz, 1H), 4.16 (q, J = 7.1 Hz, 2H), 3.75 (t, J = 4.8 Hz, 1H), 3.66–3.45 (m, 3H), 3.34 (dd, J = 14.2, 5.1 Hz, 1H), 3.17 (dd, J = 14.2, 4.4 Hz, 1H), 3.09 (dd, J = 12.5, 3.9 Hz, 1H), 2.88 (dd, J = 12.5, 4.8 Hz, 1H), 2.72 (dd, J = 14.2, 5.4 Hz, 1H), 2.56 (dd, J = 14.2, 8.9 Hz, 1H), 1.27 (t, J = 7.1 Hz, 3H); ^{13}C NMR (101 MHz, $CDCl_3$) δ 170.8, 170.4, 138.1, 136.4, 130.4, 128.1, 127.1, 126.5, 123.0, 122.2, 119.5, 118.5, 111.3, 111.2, 64.5, 60.7, 55.4, 51.1, 50.7, 35.7, 30.5, 14.2; ESI HRMS (*m/z*): calcd for $C_{24}H_{28}N_3O_3^+$ $[M+H]^+$: 406.2125, found: 406.2125.

4.27. Methyl ((S)-2-((tert-butoxycarbonyl)amino)-3-(1H-indol-3-yl) propyl)-L-tryptophanate **36**

A mixture of **34** (500 mg, 1.74 mmol), L-H-Trp-OMe x HCl (443 mg, 1.0 eq., 1.74 mmol), TEA (242 μL, 1.0 eq., 1.74 mmol) and dry THF (20 mL) was stirred at rt for 30 min. AcOH (100 μL, 1.0 eq., 1.74 mmol) and $NaBH(OAc)_3$ (552 mg, 1.5 eq., 2.60 mmol) were added and the mixture was stirred at rt overnight. AcOEt (50 mL) and 2 M aqueous solution of NaOH (20 mL) were added, and the mixture was stirred vigorously for 20 min. The layers were separated and the aqueous phase was extracted with AcOEt (15 mL). The combined organic extracts were washed with water (25 mL), saturated aqueous solution of NaCl (20 mL), dried over anhydrous Na_2SO_4, filtered and evaporated *in vacuo*. The residue was subjected to CC (manual, SiO_2, *n*-hexane/AcOEt 3:1 to 1:2) to give **36** (580 mg, 68%). Beige solid; ^{1}H NMR (400 MHz, $CDCl_3$) δ 8.22 (bs, 1H), 7.99 (bs, 1H), 7.62 (d, J = 7.9 Hz, 1H), 7.52 (d, J = 7.9 Hz, 1H), 7.36 (d, J = 8.0 Hz, 1H), 7.30 (d, J = 8.1 Hz, 1H), 7.26–7.10 (m, 3H), 7.03 (t, J = 7.7 Hz, 1H), 6.96 (d, J = 2.4 Hz, 1H), 6.54 (d, J = 2.3 Hz, 1H), 4.97 (bs, 1H), 3.93 (bs, 1H), 3.65 (s, 3H), 3.60–3.54 (m, 1H), 3.19 (dd, J = 14.4, 5.3 Hz, 1H), 3.05 (dd, J = 14.4, 7.9 Hz, 1H), 3.05–2.89 (m, 1H), 2.78 (dd, J = 14.4, 7.9 Hz, 1H), 2.65 (dd, J = 12.2, 4.9 Hz, 1H), 2.50–2.37 (m, 1H), 1.44 (s, 9H); ^{13}C NMR (101 MHz, $CDCl_3$) δ 175.2, 155.8, 136.3, 136.1, 127.8 (bs), 127.5, 123.1, 122.6, 122.1, 121.9, 119.5, 119.3, 119.0 (bs), 118.8, 111.8, 111.3, 111.2, 111.0, 79.1 (bs), 62.2, 51.8, 50.8 (bs), 50.0 (bs), 29.0, 28.5 (bs), 27.9 (bs). Broadened, low intensity signals are observed in the carbon spectrum due to the dynamic processes. ESI HRMS (*m/z*): calcd for $C_{28}H_{35}N_4O_4^+$ $[M+H]^+$: 491.2653, found: 491.2650.

4.28. Methyl N-((S)-2-((tert-butoxycarbonyl)amino)-3-(1H-indol-3-yl) propyl)-N-(2-ethoxy-2-oxoethyl)-L-tryptophanate **38**

A solution of **36** (250 mg, 0.51 mmol), DIPEA (197 μL, 3.0 eq., 0.51 mmol) and ethyl bromoacetate (256 μL, 2.0 eq., 1.86 mmol) in ACN was stirred at 50° for 3 h. Another portion of DIPEA (486 μL, 3.0 eq., 2.79 mmol) and ethyl bromoacetate (206 μL, 2.0 eq., 1.86 mmol) was added and the stirring was continued overnight. The mixture was evaporated *in vacuo* and the residue was subjected to CC (manual, SiO_2, petroleum ether/AcOEt 5:1 to 3:2) to give **38** (212 mg, 78%). White solid; ^{1}H NMR (400 MHz, $CDCl_3$) δ 7.97 (bs, 1H), 7.91 (bs, 1H), 7.56 (d, J = 7.9 Hz, 1H), 7.50 (d, J = 7.9 Hz, 1H), 7.33 (dt, J = 8.1, 1.0 Hz, 1H), 7.29 (dt, J = 8.1, 0.9 Hz, 1H), 7.21–7.13 (m, 2H), 7.12–7.04 (m, 2H), 7.00 (bs, 1H), 6.79 (bs, 1H), 5.22 (bs, 1H), 4.14 (qd, J = 7.2, 1.9 Hz, 2H), 3.90 (bs, 1H), 3.79–3.71 (m, 1H), 3.61–3.57 (m, 5H), 3.19 (dd, J = 14.5, 7.9 Hz, 1H), 3.03–2.85 (m, 4H), 2.72 (dd, J = 13.6, 7.2 Hz, 1H), 1.41 (s, 9H), 1.25 (t, J = 7.1 Hz, 3H); ^{13}C NMR (101 MHz, $CDCl_3$) δ 173.0, 172.2, 156.0, 136.2, 136.1, 128.0 (bs), 127.3, 123.1 (bs), 122.5, 121.9, 121.8, 119.4, 119.3, 119.2 (bs), 118.4, 112.4, 111.7, 111.2, 111.0 (bs), 78.9 (bs), 65.5 (bs), 60.7, 56.4 (bs), 54.0 (bs), 52.9 (bs), 51.5, 50.3 (bs), 28.4, 25.3 (bs), 14.2. Broadened, low intensity signals are observed in the carbon spectrum due to the dynamic processes; ESI HRMS (*m/z*): calcd for $C_{31}H_{39}N_4O_6^+$ $[M+H]^+$: 563.2864, found: 563.2864.

4.29. Methyl (S)-2-((S)-3-((1H-indol-3-yl)methyl)-5-oxopiperazin-1-yl)-3-(1H-indol-3-yl)propanoate **12** and ethyl 2-((2S,5S)-2,5-bis((1H-indol-3-yl)methyl)-3-oxopiperazin-1-yl)acetate **40**

A mixture of **38** (225 mg, 0.39 mmol) and 4 M solution of HCl in 1,4-dioxane (4 mL) was stirred at rt for 1 h. Argon was bubbled through the mixture followed by evaporation *in vacuo*. The residue was partitioned between AcOEt (10 mL) and saturated aqueous solution of $NaHCO_3$ (10 mL). The layers were separated and the aqueous phase was washed with AcOEt (5 mL). The combined organic fraction was washed with saturated aqueous solution of NaCl (5 mL), dried, filtered and evaporated *in vacuo*. The residue was subjected to CC (automated, 4 g, SiO_2, petroleum ether/AcOEt 4:1 to 0:1) to give **12** (120 mg, 71%) and **40** (32 mg, 18%). **12**: White solid; Purity: 95.3% (LC-MS); ^{1}H NMR (400 MHz, $CDCl_3$) δ 8.29 (s, 1H), 8.17 (s, 1H), 7.64–7.59 (m, 1H), 7.49–7.42 (m, 1H), 7.37–7.32 (m, 2H), 7.24–7.05 (m, 4H), 6.99 (d, J = 2.4 Hz, 1H), 6.75 (d, J = 2.4 Hz, 1H), 5.94 (s, 1H), 3.74–3.62 (m, 5H), 3.47 (d, J = 5.5 Hz, 2H), 3.31 (dd, J = 14.7, 7.9 Hz, 1H), 3.21 (dd, J = 12.1, 4.0 Hz, 1H), 3.14 (dd, J = 14.6, 7.3 Hz, 1H), 2.95 (dd, J = 14.2, 5.7 Hz, 1H), 2.73 (dd, J = 14.2, 8.9 Hz, 1H), 2.56 (dd, J = 12.0, 7.3 Hz, 1H); ^{13}C NMR (101 MHz, $CDCl_3$) δ 171.9, 169.2, 136.5, 136.1, 127.3, 127.0, 123.1, 122.7, 122.4, 122.1, 119.6, 119.5, 118.5, 118.4, 111.5, 111.4, 111.4, 110.4, 66.3, 53.8, 52.1, 51.4, 50.6, 30.3, 25.2; ESI HRMS (*m/z*): calcd for $C_{25}H_{27}N_4O_3^+$ $[M+H]^+$: 431.2078, found: 431.2079. **40**: Beige solid; ^{1}H NMR (400 MHz, $CDCl_3$) δ 8.35 (bs, 1H), 8.19 (bs, 1H), 7.80 (d, J = 7.2 Hz, 1H), 7.42–7.08 (m, 7H), 7.04 (t, J = 7.5 Hz, 1H), 6.34 (d, J = 2.5 Hz, 1H), 5.98 (d, J = 3.2 Hz, 1H), 4.15 (q, J = 7.1 Hz, 2H), 3.78 (t, J = 4.5 Hz, 1H), 3.68–3.51 (m, 4H), 3.30 (dd, J = 15.2, 4.3 Hz, 1H), 3.06 (dd, J = 12.4, 4.0 Hz, 1H), 2.88 (dd, J = 12.3, 4.8 Hz, 1H), 2.67 (dd, J = 14.1, 5.3 Hz, 1H), 2.49 (dd, J = 14.1, 8.9 Hz, 1H), 1.26 (t, J = 7.1 Hz, 3H); ^{13}C NMR (101 MHz, $CDCl_3$) δ 171.6, 170.7, 136.3, 136.0, 128.1, 127.0, 123.9, 123.1, 122.0, 121.7, 119.6, 119.40, 119.37, 118.4, 111.9, 111.3, 111.1, 110.9, 64.1, 60.7, 55.4, 51.0, 50.6, 30.4, 25.7, 14.2; ESI HRMS (*m/z*): calcd for $C_{26}H_{29}N_4O_3^+$ $[M+H]^+$: 445.2234, found: 445.2234.

4.30. tert-Butyl ((S)-1-(((S)-1-hydroxy-3-(1H-indol-3-yl)propan-2-yl)amino)-3-(1H-indol-3-yl)propan-2-yl)carbamate **41**

A mixture of L-H-Trp-ol (1.01 g, 1.0 eq., 5.31 mmol), **34** (1.53 g, 5.31 mmol), AcOH (0.30 mL, 1.0eq., 5.31 mmol), $NaBH(OAc)_3$ (1.69 g, 1.5 eq., 7.96 mmol) and dry THF (40 mL) was stirred at rt overnight. AcOEt (150 mL) and saturated aqueous solution of $NaHCO_3$ (100 mL) were added, and the mixture was stirred vigorously for 30 min. The layers were separated and the aqueous phase was extracted with AcOEt (40 mL). The combined organic extracts were washed with water (75 mL), saturated aqueous solution of NaCl (75 mL), dried over anhydrous Na_2SO_4, filtered and evaporated *in vacuo*. The residue was subjected to CC (automated, 40 g, SiO_2, AcOEt/MeOH/TEA 99:0:1 to 90:9:1) to give **41** (1.20 g, 49%). White solid; ^{1}H NMR (400 MHz, DMSO) δ 10.79–10.71 (m, 2H), 7.57–7.50 (m, 1H), 7.47–7.41 (m, 1H), 7.34–7.27 (m, 2H), 7.09–6.98 (m, 4H), 6.98–6.88 (m, 2H), 6.62 (d, J = 8.3 Hz, 1H), 4.43–4.31 (m, 1H), 3.71 (q, J = 6.7 Hz, 1H), 3.33–3.17 (m, 2H), 2.83–2.54 (m, 7H), 1.34 (s, 9H); ^{13}C NMR (101 MHz, DMSO) δ 155.9, 136.7, 136.6, 128.03, 128.00, 123.7, 123.5, 121.2, 119.0, 118.8, 118.60, 118.55, 112.1, 112.0, 111.74, 111.70, 77.8, 63.5, 60.4, 51.9, 50.4, 49.1, 28.7, 27.3; ESI HRMS (*m/z*): calcd for $C_{27}H_{35}N_4O_3^+$ $[M+H]^+$: 463.2704, found: 463.2705.

4.31. tert-butyl ((S)-1-((S)-5-((1H-indol-3-yl)methyl)-2-oxomorpholino)-3-(1H-indol-3-yl)propan-2-yl)carbamate **43** and (S)-6-((1H-indol-3-yl)methyl)-4-((S)-1-hydroxy-3-(1H-indol-3-yl)propan-2-yl)piperazin-2-one **14**

A solution of **41** (500 mg, 1.08 mmol), DIPEA (486 μL, 3.0 eq., 2.79 mmol) and ethyl bromoacetate (309 μL, 3.0 eq., 2.79 mmol) in ACN was stirred at 60° for 7 h. The mixture was evaporated *in vacuo* and subjected to CC (automated, 12 g, SiO_2, *n*-hexane/AcOEt 3:1 to 0:1) to give **42** (383 mg, 66%, LC-MS (*m/z*)) that did not give satisfactory NMR spectra and **43** (54 mg, 10%). **43**: White solid, ^{1}H NMR (400 MHz, $CDCl_3$) δ 8.15 (bs, 1H), 8.09 (bs, 1H), 7.67–7.59 (m, 1H), 7.47–7.30 (m, 3H), 7.24–7.05 (m, 4H), 6.96–6.93 (m, 1H), 6.84 (d, J = 2.4 Hz, 1H), 4.61 (bs, 1H), 4.28–4.03 (m, 3H), 3.70–3.42 (m, 2H), 3.18–3.10 (m, 1H), 3.08–2.95 (m, 2H), 2.89 (dd, J = 14.3, 4.5 Hz, 1H), 2.82–2.66 (m, 2H), 2.58 (dd, J = 12.8, 8.4 Hz, 1H), 1.45 (s, 9H); ^{13}C NMR (101 MHz, $CDCl_3$) δ 168.8, 155.8, 136.22, 136.22, 127.9, 127.1, 122.9, 122.8, 122.7, 122.23, 122.16, 119.68, 119.63, 119.0, 118.4, 111.4, 111.2, 79.5, 70.5, 70.2, 57.1, 55.9, 51.7, 48.6, 29.7, 28.4, 21.4. LC-MS (*m/z*): 503 $[M+H]^+$. The crude **42** (350 mg, 0.71 mmol) was dissolved in 4 M solution of HCl in 1,4-dioxane (6 mL) and the solution was stirred at rt for 1 h. Argon was bubbled through the mixture followed by evaporation *in vacuo*. The residue was dissolved in MeOH (4 mL) and TEA (396 μL, 4.0 eq., 2.84 mmol) and stirred overnight at rt. The mixture was evaporated *in vacuo* and the crude was purified by CC (automated, 4g, RP-C18, water/CH_3CN gradient) to give **14** (151 mg, 53%). Beige solid; Purity: 96.1% (LC-MS); ^{1}H NMR (400 MHz, DMSO) δ 10.82 (d, J = 2.4 Hz, 1H), 10.76 (d, J = 2.3 Hz, 1H), 7.75 (d, J = 2.2 Hz, 1H), 7.49–7.39 (m, 2H), 7.32 (dt, J = 4.5, 0.9 Hz, 1H), 7.30 (dt, J = 4.5, 0.9 Hz, 1H), 7.09 (d, J = 2.4 Hz, 1H), 7.07–6.99 (m, 2H), 6.98–6.87 (m, 3H), 4.33 (t, J = 5.2 Hz, 1H), 3.52–3.42 (m, 2H), 3.41–3.30 (m, 1H), 3.30–3.15 (m, 2H), 2.85–2.70 (m, 5H), 2.66–2.53 (m, 2H); ^{13}C NMR (101 MHz, DMSO) δ 169.0, 136.6, 127.75, 127.72, 124.0, 123.7, 121.3, 121.2, 118.77, 118.76, 118.66, 118.60, 112.7, 111.84, 111.82, 111.0, 65.5, 60.8, 53.3, 52.5, 49.8, 40.6, 40.4, 40.2, 40.0, 39.7, 39.5, 39.3, 30.2, 22.6; ESI HRMS (*m/z*): calcd for $C_{24}H_{27}N_4O_2^+$ $[M+H]^+$: 403.2128, found: 403.2130.

4.32. (S)-2-((S)-3-((1H-indol-3-yl)methyl)-5-oxopiperazin-1-yl)-3-(1H-indol-3-yl)propyl acetate **15**

A solution of **14** (90 mg, 224 μmol) and DMAP (1 mg, 0.05 eq., 13 μmol) in dry THF (1 mL) was cooled (0 °C). DIPEA (47 μL, 1.5 eq., 336 μmol) and Ac_2O (35 μL, 1.2 eq., 173 μmol) were added and the resulting mixture was allowed to reach rt and stirred overnight. The solution was evaporated *in vacuo* and The residue was subjected to CC (manual, SiO_2, *n*-hexane/AcOEt 3:1 to 1/2), to give **15** (68 mg, 68%). White solid; Purity: 98.2% (LC-MS); ^{1}H NMR (400 MHz, $CDCl_3$) δ ^{1}H NMR (400 MHz, $CDCl_3$) δ 8.22 (bs, 1H), 8.12 (bs, 1H), 7.58 (d, J = 7.8 Hz, 1H), 7.49 (d, J = 7.8 Hz, 1H), 7.39–7.33 (m, 2H), 7.24–7.18 (m, 2H), 7.17–7.06 (m, 2H), 7.00 (d, J = 2.2 Hz, 1H), 6.77 (d, J = 2.2 Hz, 1H), 5.94 (bs, 1H), 4.22 (dd, J = 11.8, 7.2 Hz, 1H), 4.18–4.03 (m, 1H), 3.81–3.68 (m, 1H), 3.55 (d, J = 16.3 Hz, 1H), 3.47 (d, J = 16.5 Hz, 1H), 3.33–3.23 (m, 1H), 3.16–2.98 (m, 2H), 2.93 (dd, J = 14.2, 5.9 Hz, 1H), 2.88–2.72 (m, 2H), 2.63 (dd, J = 11.7, 6.6 Hz, 1H), 2.03 (s, 3H); ^{13}C NMR (101 MHz, $CDCl_3$) δ 170.9, 169.6, 136.5, 136.3, 127.3, 127.0, 123.0, 122.6, 122.4, 122.1, 119.7, 119.5, 118.53, 118.49, 112.5, 111.43, 111.38, 110.7, 63.55, 61.63, 53.2, 52.2, 50.9, 30.4, 23.7, 21.0; ESI HRMS (*m/z*): calcd for $C_{26}H_{29}N_4O_3^+$ $[M+H]^+$: 445.2234, found: 445.2234.

4.33. Methyl ((S)-2-(2-ethoxy-2-oxoacetamido)-3-(1H-indol-3-yl)propyl)-L-tryptophanate **44**

A mixture of **36** (80 mg, 163 μmol) and 4 N HCl solution in 1,4-dioxane (1 mL) was stirred at rt for 1 h. The mixture was concentrated *in vacuo*. The resulting crude methyl ((*S*)-2-amino-3-(1*H*-indol-3-yl) propyl)-L-tryptophanate hydrochloride was dissolved in EtOH (0.5 mL). TEA (45 μL, 2.0 eq., 326 μmol) and $(COOEt)_2$ (221 μL, 10.0 eq., 1.63 mmol) were added and the mixture was refluxed for 10 h. The solution was concentrated *in vacuo* and the residue was purified by CC (automated, 4g, RP-C18, water/CH_3CN gradient) to give **44** (41 mg, 51%). White solid; ^{1}H NMR (400 MHz, CD_3OD) δ 7.51 (q, J = 1.0 Hz, 1H), 7.49 (q, J = 1.0 Hz, 1H), 7.33 (dt, J = 8.1, 0.9 Hz, 1H), 7.29 (dt, J = 8.1, 0.9 Hz, 1H), 7.13–7.02 (m, 3H), 7.00 (ddd, J = 8.0, 7.0, 1.0 Hz, 1H), 6.94 (ddd, J = 8.0, 7.0, 1.0 Hz, 1H), 6.84 (s, 1H), 4.31–4.16 (m, 3H),

3.59–3.52 (m, 4H), 3.13 (ddd, J = 14.2, 6.2, 0.6 Hz, 1H), 3.01 (ddd, J = 14.4, 7.6, 0.6 Hz, 1H), 2.96–2.80 (m, 2H), 2.75 (dd, J = 12.3, 4.6 Hz, 1H), 2.58 (dd, J = 12.3, 7.4 Hz, 1H), 1.30 (t, J = 7.1 Hz, 3H); ^{13}C NMR (101 MHz, CD_3OD) δ 174.9, 159.9, 157.6, 136.7, 136.6, 127.4, 127.2, 123.1, 122.7, 121.1, 120.9, 118.5, 118.3, 118.0, 117.8, 111.0, 110.8, 110.3, 109.6, 62.4, 62.1, 51.1, 50.8, 49.7, 28.4, 27.4, 12.8; LC-MS (m/z): 491 $[M+H]^+$.

4.34. Methyl (S)-2-((S)-5-((1H-indol-3-yl)methyl)-2,3-dioxopiperazin-1-yl)-3-(1H-indol-3-yl)propanoate **13**

A mixture of **44** (30 mg, 61 μmol), TEA (26 μL, 3.0 eq., 183 μmol) and toluene (0.5 mL) was refluxed for 16 h and evaporated *in vacuo*. The residue was purified by CC (automated, 4g, RP-C18, water/CH_3CN gradient) to give **13** (22 mg, 81%). White solid; Purity: 95.7% (LC-MS); ^{1}H NMR (400 MHz, CD_3OD) δ 7.48 (d, J = 7.9 Hz, 1H), 7.37–7.29 (m, 3H), 7.14–7.07 (m, 2H), 7.04–6.97 (m, 2H), 6.83 (s, 1H), 6.75 (s, 1H), 5.15 (dd, J = 10.9, 5.4 Hz, 1H), 3.73 (s, 3H), 3.56–3.32 (m, 4H), 3.22 (dd, J = 12.6, 7.1 Hz, 1H), 2.78 (dd, J = 14.3, 6.0 Hz, 1H), 2.59 (dd, J = 14.3, 8.1 Hz, 1H); ^{13}C NMR (101 MHz, CD_3OD) δ 170.4, 158.6, 157.6, 136.71, 136.65, 126.99, 126.95, 123.4, 123.0, 121.3, 121.2, 118.7, 118.6, 117.7, 117.6, 111.2, 111.0, 109.1, 108.8, 59.4, 51.6, 49.9, 47.9, 28.2, 23.8; LC-MS (m/z): 445 $[M+H]^+$.

4.35. Methyl (S)-(2-((tert-butoxycarbonyl)amino)-3-(1H-indol-3-yl) propyl)glycinate **45**

A mixture of **34** (7.00 g, 24.28 mmol), Gly-OMe x HCl (3.05 g, 1.0 eq., 24.28 mmol), TEA (3.28 mL, 1.0 eq., 24.28 mmol), dry CH_2Cl_2 (100 mL) and MeOH (50 mL) was stirred at rt for 30 min. AcOH (1.39 mL, 1.0 eq., 24.28 mmol) was added, followed by $NaBH_3CN$ (2.29 g, 1.5 eq., 36.42 mmol) and the mixture was stirred at rt overnight. CH_2Cl_2 (250 mL) was added, followed by saturated aqueous solution of $NaHCO_3$ (150 mL). The mixture was stirred vigorously for 20 min. The layers were separated and the aqueous phase was extracted with DCM (2 × 75 mL). The combined organic extracts were washed with water (150 mL), saturated aqueous solution of NaCl (150 mL), dried over anhydrous Na_2SO_4, filtered and evaporated *in vacuo*. The residue was subjected to CC (manual, SiO_2, *n*-hexane/AcOEt 3:1 to 0:1) to give **45** (6.81 g, 77%). Beige solid; ^{1}H NMR (400 MHz, DMSO) δ 10.75 (d, J = 2.0 Hz, 1H), 7.54 (d, J = 7.8 Hz, 1H), 7.30 (dt, J = 8.1, 1.0 Hz, 1H), 7.07 (d, J = 2.2 Hz, 1H), 7.03 (ddd, J = 8.1, 7.0, 1.2 Hz, 1H), 6.94 (ddd, J = 7.9, 7.0, 1.0 Hz, 1H), 6.61 (d, J = 8.3 Hz, 1H), 3.74–3.65 (m, 1H), 3.57 (s, 3H), 3.28 (d, J = 2.2 Hz, 2H), 2.84–2.71 (m, 2H), 2.53–2.49 (m, 2H), 2.00 (bs, 1H), 1.34 (s, 9H);^{13}C NMR (101 MHz, DMSO) δ 173.1, 155.9, 136.6, 128.0, 123.6, 121.2, 118.9, 118.6, 111.8, 111.7, 79.6, 77.9, 52.2, 51.7, 51.5, 50.6, 28.71; ESI HRMS (m/z): calcd for $C_{19}H_{28}N_4O_3^+$ $[M+H]^+$: 362.2074, found: 362.2072.

4.36. (S)-6-((1H-indol-3-yl)methyl)piperazin-2-one **46**

Compound **45** (3.20 g, 9.57 mmol) was dissolved in 4 M solution of HCl in 1,4-dioxane (50 mL) and the solution was stirred at rt for 1 h. Argon was bubbled through the mixture followed by evaporation *in vacuo*. The residue was dissolved in MeOH (50 mL) and TEA (1.60 mL, 1.2 eq., 11.49 mmol) and stirred overnight at rt. The mixture was evaporated *in vacuo* and the crude was purified by CC (automated, 24g, RP-C18, water/CH_3CN gradient) to give **46** (0.96 g, 44%). Beige solid; ^{1}H NMR (400 MHz, $CDCl_3$) δ 8.62 (bs, 1H), 7.58–7.51 (m, 1H), 7.37 (dt, J = 8.2, 0.9 Hz, 1H), 7.21 (ddd, J = 8.1, 7.0, 1.1 Hz, 1H), 7.13 (ddd, J = 8.0, 7.0, 1.0 Hz, 1H), 6.99 (d, J = 2.3 Hz, 1H), 6.02 (bs, 1H), 3.82–3.70 (m, 1H), 3.57–3.41 (m, 2H), 3.23 (dd, J = 13.0, 4.2 Hz, 1H), 3.02 (ddd, J = 14.2, 4.9, 0.8 Hz, 1H), 2.82–2.69 (m, 2H), 1.81 (bs, 1H); ^{13}C NMR (101 MHz, $CDCl_3$) δ 170.1, 136.6, 127.0, 123.1, 122.4, 119.7, 118.4, 111.6, 110.0, 53.1, 49.6, 48.2, 30.4; LC-MS (m/z): 230 $[M+H]^+$.

4.37. (S)-4-(2-(1H-indol-3-yl)ethyl)-6-((1H-indol-3-yl)methyl) piperazin-2-one **16**

3-indoleacetaldehyde was synthesized as described [31] and was used immediately without further characterization. A solution of **46** (38 mg, 165 μmol), 3-indoleacetaldehyde (53 mg, 2.0 eq., 330 μmol), AcOH (9 μL, 1.0 eq., 165 μmol) in dry THF (1 mL) was stirred at rt for 15 min. $NaBH(OAc)_3$ (53 mg, 1.5 eq., 248 μmol) and the mixture was stirred at rt overnight. AcOEt (10 mL) was added, followed by saturated aqueous solution of $NaHCO_3$ (10 mL). The mixture was stirred vigorously for 20 min. The layers were separated and the aqueous phase was extracted with AcOEt (2 × 2 mL). The combined organic extracts were washed with water (5 mL), saturated aqueous solution of NaCl (5 mL), dried over anhydrous Na_2SO_4, filtered and evaporated *in vacuo*. The residue was subjected to CC (automated, SiO_2, CH_2Cl_2 to CH_2Cl_2/MeOH 95:5) to give **16** (54 mg, 73%). Beige solid; Purity: 95.7% (LC-MS); ^{1}H NMR (400 MHz, CD_3OD) δ 7.52 (dt, J = 7.9, 0.9 Hz, 1H), 7.47 (dt, J = 7.9, 1.0 Hz, 1H), 7.34 (dt, J = 8.2, 0.9 Hz, 1H), 7.30 (dt, J = 8.1, 0.9 Hz, 1H), 7.14–7.03 (m, 2H), 7.02–6.93 (m, 4H), 3.82–3.71 (m, 1H), 3.21 (d, J = 16.6 Hz, 1H), 3.11 (d, J = 16.6 Hz, 1H), 3.04–2.94 (m, 2H), 2.93–2.85 (m, 2H), 2.78 (ddd, J = 11.9, 4.2, 1.0 Hz, 1H), 2.74–2.64 (m, 2H), 2.43 (dd, J = 11.9, 7.1 Hz, 1H); ^{13}C NMR (101 MHz, CD_3OD) δ 170.5, 136.7, 136.7, 127.3, 127.3, 123.1, 121.8, 121.1, 120.8, 118.5, 118.1, 117.9, 117.8, 112.3, 111.0, 110.8, 109.8, 57.7, 56.0, 53.3, 52.1, 29.6, 22.3; LC-MS (m/z): 373 $[M+H]^+$.

4.38. (S)-4-(2-(1H-indol-3-yl)acetyl)-6-((1H-indol-3-yl)methyl) piperazin-2-one **17**

A solution of **46** (150 mg, 0.66 mmol) and DMAP (4 mg, 0.05 eq., 33 μmol) in DMF (2 mL) was cooled (0 °C). DIPEA (228 μL, 2.0 eq., 1.31 mmol), (1*H*-indol-3-yl)acetic acid (115 mg, 1.0 eq., 0.66 mmol) and EDC (208 mg, 1.5 eq., 0.98 mmol) were added and the resulting mixture was allowed to reach rt and stirred overnight. The mixture was poured on water (10 mL) and extracted with AcOEt (3 × 5 mL). The combined organic extract was washed with saturated aqueous solution of NH_4Cl (5 × 5 mL), dried over anhydrous Na_2SO_4, filtered and evaporated *in vacuo*. The residue was subjected to CC (automated, 4g, RP-C18, water/CH_3CN gradient), to give **17** (110 mg, 44%). White solid; Purity: 97.8% (LC-MS); ^{1}H NMR (400 MHz, rotamers, CD_3OD) δ 7.59 (dt, J = 7.9, 1.0 Hz, 1 H_{minor}), 7.45 (dt, J = 7.8, 1.0 Hz, 1H_{minor}), 7.40 (dt, J = 8.1, 0.9 Hz, 1H_{major}), 7.38–7.26 (m, 4H_{major} and 3H_{minor}), 7.20–7.14 (m, 1H_{minor}), 7.14–7.12 (m, 1H_{major}), 7.12–7.03 (m, 4H_{minor}), 7.03–6.99 (m, 1H_{major}), 6.99–6.91 (m, 1H_{major} and 2H_{minor}), 6.60 (s, 1H_{major}), 4.33 (d, J = 18.4 Hz, 1H_{major}), 4.20 (d, J = 17.7 Hz, 1H_{minor}), 4.09 (d, J = 17.7 Hz, 1H_{minor}), 3.92–3.69 (m, 3H_{major} and 3H_{minor}), 3.69–3.62 (m, 1H_{minor}), 3.62–3.54 (m, 1H_{major} and 1H_{minor}), 3.47–3.37 (m, 1H_{major}), 3.24 (dd, J = 13.7, 7.9 Hz, 1H_{major}), 2.92–2.81 (m, 1H_{major} and 1H_{minor}), 2.81–2.64 (m, 1H_{major} and 1H_{minor}); ^{13}C NMR (101 MHz, rotamers, CD_3OD) δ 171.8, 171.7, 168.4, 167.7, 136.74, 136.68, 136.5, 127.19, 127.14, 126.9, 126.6, 123.6, 123.2, 123.0, 122.7, 121.4, 121.32, 121.30, 121.0, 118.72, 118.68, 118.5, 118.1, 117.9, 117.79, 117.76, 111.1, 111.0, 110.9, 109.2, 108.8, 106.9, 106.8, 51.6, 51.3, 48.31, 46.6, 45.2, 41.5, 31.2, 31.1, 29.2, 28.5; ESI HRMS (m/z): calcd for $C_{23}H_{23}N_4O_2^+$ $[M+H]^+$: 387.1816, found: 387.1816.

4.39. 4-(S)-benzyl-3-tert-butyl-1,2,3-oxathiazolidine-3,4-dicarboxylate-2,2-dioxide **47**

To a cooled (0 °C), stirred solution of imidazole (13.83 g, 203.4 mmol) in dry CH_2Cl_2 (160 mL) was added a solution of $SOCl_2$ (4.92 mL, 0.33 eq., 67.8 mmol) in dry CH_2Cl_2 (20 mL), dropwise, over 30 min. The mixture was then allowed to reach rt, stirred for 30 min and cooled (−78 °C). Subsequently, a solution of L-Boc-Ser-OBn (10.00g, 0.13 eq., 33.90 mmol) in dry CH_2Cl_2 (40 mL) was added, dropwise, over 30 min. The mixture was stirred at −78 °C for further 10 min, after which it was

brought to room temperature and stirred for 1 h. 1 M aqueous solution of citric acid (300 mL) and the mixture was shaken in a separatory funnel. The layers were separated and the aqueous phase was washed with CH_2Cl_2 (3 × 50 mL). The combined organic extracts were washed with water (75 mL), saturated aqueous solution of NaCl (75 mL), dried over anhydrous Na_2SO_4, filtered and evaporated *in vacuo*. The resulting crude 4-(*S*)-benzyl-3-*tert*-butyl-1,2,3-oxathiazolidine-3,4-dicarboxylate-2,2-oxide was dissolved in CH_3CN (70 mL) and the solution was cooled to 0 °C. Subsequently, $RuCl_3xH_2O$ (38.0 mg, 0.005 eq., 170 μmol) and $NaIO_4$ (7.29 g, 1.0 eq., 33.90 mmol) were added. The mixture was allowed to reach rt and stirred for 1 h. Water (70 mL) and AcOEt (120 mL) were added and the mixture was shaken in a separatory funnel. The layers were separated and the aqueous phase was extracted with AcOEt (3 × 30 mL). The combined organic extracts were washed with saturated aqueous solution of $NaHCO_3$ (70 mL), water (70 mL) and saturated aqueous solution of NaCl (70 mL), dried over anhydrous Na_2SO_4, filtered and evaporated *in vacuo*. The residue was dissolved in a 1:1 mixture of CH_2Cl_2/Et_2O and kept in the freezer. The crystals were filtered and dried to give **47** (10.43 g, 86%). White crystals, ^{1}H NMR (400 MHz, $CDCl_3$) δ 7.42–7.30 (m, 5H), 5.32 (d, J = 12.1 Hz, 1H), 5.22 (d, J = 12.1 Hz, 1H), 4.86–4.79 (m, 1H), 4.76 (dd, J = 9.4, 6.7 Hz, 1H), 4.66 (dd, J = 9.4, 2.0 Hz, 1H), 1.49 (s, 9H); ^{13}C NMR (101 MHz, $CDCl_3$) δ 166.9, 148.0, 134.4, 128.8, 128.7, 128.4, 86.3, 68.5, 67.4, 57.6, 27.8.

4.40. Methyl (2-methoxy-2-oxoethyl)-L-tryptophanate **48**

L-H-Trp-OMe x HCl (5.00 g, 19.6 mmol) was dissolved in CH_3CN (60 mL). DIPEA (9.47 mL, 2.5 eq., 54.5 mmol) was added followed by dropwise addition of methyl bromoacetate (2.25 mL, 1.2 eq., 23.5 mmol). The solution was stirred at rt overnight and concentrated *in vacuo*. The residue was partitioned between AcOEt (75 mL) and water (50 mL). The phases were separated and the aqueous phase was washed with AcOEt (40 mL). The combined organic layers were washed with saturated aqueous solution of NH_4Cl (50 mL), dried over anhydrous Na_2SO_4, filtered and concentrated *in vacuo*. The residue was subjected to CC (manual, SiO_2, cyclohexane/AcOEt 4:1 to 1:1) to give **48** (5.69, 88%). Pale-yellow oil; ^{1}H NMR (400 MHz, $CDCl_3$) δ 8.20 (bs, 1H), 7.60 (ddd, J = 7.8, 1.3, 0.6 Hz, 1H), 7.34 (dt, J = 8.1, 1.0 Hz, 1H), 7.18 (ddd, J = 8.2, 7.1, 1.2 Hz, 1H), 7.11 (ddd, J = 8.1, 7.0, 1.1 Hz, 2H), 7.09 (d, J = 2.4 Hz, 1H), 3.70 (dd, J = 7.3, 5.8 Hz, 1H), 3.66 (s, 3H), 3.63 (s, 3H), 3.47 (d, J = 17.2 Hz, 1H), 3.35 (d, J = 17.2 Hz, 1H), 3.25 (ddd, J = 14.5, 5.8, 0.8 Hz, 1H), 3.14 (ddd, J = 14.5, 7.3, 0.7 Hz, 1H), 2.11 (bs, 1H); ^{13}C NMR (101 MHz, $CDCl_3$) δ 174.4, 172.2, 136.2, 127.4, 123.0, 122.1, 119.4, 118.7, 111.2, 110.8, 61.1, 51.9, 51.8, 49.1, 29.2; LC-MS (*m/z*): 291 $[M+H]^+$.

4.41. Benzyl (S)-4-((S)-3-(1H-indol-3-yl)-1-methoxy-1-oxopropan-2-yl)-6-oxopiperazine-2-carboxylate **49**

A mixture of **48** (579 mg, 2.00 mmol) and **47** (950 mg, 1.33 eq., 2.66 mmol) in CH_3CN (30 mL) was stirred at 70 °C overnight. The mixture was concentrated *in vacuo* and the crude intermediate (LC/MS (ESI+): 568 $[M\text{-}SO_3H+H]^+$) was treated with 4 N solution of HCl in 1,4-dioxane (20 mL). The mixture was stirred at rt for 1 h and concentrated *in vacuo*. The residue was partitioned between AcOEt (40 mL) and saturated aqueous solution of $NaHCO_3$ (20 mL). The phases were separated and the aqueous phase was washed with AcOEt (10 mL). The combined organic layers were washed with saturated aqueous solution of NaCl (20 mL), dried over anhydrous Na_2SO_4, filtered and concentrated *in vacuo*. The residue was subjected to CC (manual, SiO_2, cyclohexane/AcOEt 3:1 to 0:1) to give **49** (400 mg, 35%). White solid; ^{1}H NMR (400 MHz, $CDCl_3$) δ 8.07 (bs, 1H), 7.53 (ddt, J = 7.7, 1.2, 0.7 Hz, 1H), 7.35 (dt, J = 8.1, 1.0 Hz, 1H), 7.33–7.27 (m, 3H), 7.24–7.16 (m, 3H), 7.12 (ddd, J = 8.0, 7.0, 1.1 Hz, 1H), 7.00 (d, J = 2.3 Hz, 1H), 6.40 (d, J = 2.6 Hz, 1H), 5.10 (d, J = 12.0 Hz, 1H), 4.93 (d, J = 12.1 Hz, 1H), 4.12 (ddd, J = 5.0, 4.1, 2.5 Hz, 1H), 3.70–3.58 (m, 4H), 3.48 (d, J = 6.0 Hz, 2H), 3.40 (dd, J = 12.2, 5.1 Hz, 1H), 3.22 (ddd, J = 14.9, 8.1, 0.9 Hz, 1H), 3.07 (dd, J = 12.2, 4.1 Hz, 1H), 2.95 (ddd, J = 14.8, 6.9, 1.0 Hz, 1H); ^{13}C NMR (101 MHz, $CDCl_3$) δ 171.5, 170.0, 168.6, 136.0, 134.8, 128.6, 128.6, 127.2, 122.6, 122.1, 119.4, 118.5, 111.24, 111.19, 67.6, 65.9, 54.4, 54.2, 51.4, 47.3, 25.2; LC-MS (*m/z*): 436 $[M+H]^+$.

4.42. (S)-4-((S)-3-(1H-indol-3-yl)-1-methoxy-1-oxopropan-2-yl)-6-oxopiperazine-2-carboxylic acid **50**

49 (322 mg, 739 μmol) and 1,4-cyclohexadiene (419 μL, 6.0 eq., 739 μmol) were dissolved in MeOH (5 mL). Argon was passed through the solution for 20 min, followed by addition of 10% Pd/C (64,4 mg, 20% wt %). The mixture was then stirred at reflux for 4 h, cooled to rt, filtered and evaporated *in vacuo*. The residue was subjected to CC (automated, 4g, RP-C18, water/CH_3CN gradient) to give **50** (255 mg, 75%). White powder; ^{1}H NMR (400 MHz, DMSO) δ 12.82 (bs, 1H), 10.82 (d, J = 2.5 Hz, 1H), 7.94 (d, J = 3.2 Hz, 1H), 7.47 (dt, J = 7.9, 0.9 Hz, 1H), 7.34–7.27 (m, 1H), 7.09 (d, J = 2.4 Hz, 1H), 7.04 (ddd, J = 8.2, 7.0, 1.2 Hz, 1H), 6.96 (ddd, J = 8.0, 7.0, 1.1 Hz, 1H), 3.94 (q, J = 3.8 Hz, 1H), 3.61–3.54 (m, 1H), 3.51 (s, 3H), 3.25 (ddd, J = 8.4, 5.8, 2.8 Hz, 2H), 3.14–3.05 (m, 1H), 2.90–2.75 (m, 2H); ^{13}C NMR (101 MHz, DMSO) δ 173.0, 171.5, 167.8, 136.5, 127.4, 123.9, 121.4, 118.8, 118.5, 111.8, 110.1, 66.2, 54.8, 53.9, 51.5, 25.27; LC-MS (*m/z*): 346 $[M+H]^+$.

4.43. Methyl (S)-2-((S)-3-(benzylcarbamoyl)-5-oxopiperazin-1-yl)-3-(1H-indol-3-yl)propanoate **18**

A solution of **50** (68.0 mg, 197 μmol), benzylamine (24.8 mg, 1.0 eq., 232 μmol), EDC (45.4 mg, 1.2 eq., 237 μmol), HOBt (39.9 mg, 1.5 eq., 296 μmol), DIPEA (68.5 μL, 2.0 eq., 394 μmol) and DMF (1 mL) was stirred at rt overnight. The mixture was partitioned between AcOEt (5 mL) and saturated aqueous solution of NH_4Cl (2 mL). The phases were separated and the aqueous phase was washed with AcOEt (2 mL). The combined organic layers were washed with saturated aqueous solution of NH_4Cl (5 × 2 mL), dried over anhydrous Na_2SO_4, filtered and concentrated *in vacuo*. The residue was subjected to CC (automated, 4g, SiO_2, CH_2Cl_2 to CH_2Cl_2/MeOH 95:5) to give **18** (51.0 mg, 73%). White solid; Purity: 98.2% (LC-MS); ^{1}H NMR (400 MHz, $CDCl_3$) δ 8.00 (bs, 1H), 7.55–7.48 (m, 1H), 7.33–7.29 (m, 2H), 7.25–7.15 (m, 6H), 7.14–7.08 (m, 2H), 6.94 (d, J = 2.4 Hz, 1H), 4.40–4.26 (m, 2H), 3.91 (q, J = 3.7 Hz, 1H), 3.62–3.55 (m, 4H), 3.51 (dd, J = 12.3, 3.1 Hz, 1H), 3.31 (s, 2H), 3.22 (ddd, J = 14.8, 7.8, 0.8 Hz, 1H), 2.98 (ddd, J = 14.7, 6.8, 0.8 Hz, 1H), 2.86 (dd, J = 12.3, 4.3 Hz, 1H); ^{13}C NMR (101 MHz, $CDCl_3$) δ 171.6, 170.5, 169.6, 137.9, 136.1, 128.6, 127.7, 127.5, 127.1, 123.0, 122.1, 119.4, 118.4, 111.2, 111.0, 65.9, 55.8, 54.7, 51.5, 47.2, 43.5, 25.2; LC-MS (*m/z*): 435 $[M+H]^+$.

4.44. Methyl (S)-3-(1H-indol-3-yl)-2-((S)-3-((naphthalen-1-ylmethyl) carbamoyl)-5-oxopiperazin-1-yl)propanoate **19**

A solution of **50** (80.0 mg, 232 μmol), 1-naphthylmethylamine (36.42 mg, 1.0 eq., 232 μmol), EDC (52.4 mg, 1.2 eq., 278 μmol), HOBt (47.0 mg, 1.5 eq., 348 μmol), DIPEA (80.6 μL, 2.0 eq., 464 μmol) and DMF (1 mL) was stirred at rt overnight. The mixture was partitioned between AcOEt (5 mL) and saturated aqueous solution of NH_4Cl (2 mL). The phases were separated and the aqueous phase was washed with AcOEt (2 mL). The combined organic layers were washed with saturated aqueous solution of NH_4Cl (5 × 2 mL), dried over anhydrous Na_2SO_4, filtered and concentrated *in vacuo*. The residue was subjected to CC (automated, 4g, SiO_2, CH_2Cl_2 to CH_2Cl_2/MeOH 95:5) to give **19** (80.0 mg, 71%). White solid; Purity: 95.5% (LC-MS); ^{1}H NMR (400 MHz, CD_3OD) δ 8.02–7.94 (m, 1H), 7.85–7.75 (m, 1H), 7.75–7.69 (m, 1H), 7.49–7.39 (m, 4H), 7.37 (dd, J = 8.2, 7.0 Hz, 1H), 7.32 (dt, J = 8.1, 0.9 Hz, 1H), 7.09 (ddd, J = 8.1, 7.0, 1.2 Hz, 1H), 7.04–6.95 (m, 2H), 4.82–4.68 (m, 2H), 4.00 (t, J = 3.7 Hz, 1H), 3.65 (dd, J = 8.7, 6.5 Hz, 1H), 3.55 (s, 3H), 3.49–3.40 (m, 2H), 3.34 (s, 1H), 3.13 (ddd, J = 14.5,

8.7, 0.8 Hz, 1H), 2.93–2.83 (m, 2H); ^{13}C NMR (101 MHz, CD_3OD) δ 171.74, 171.73, 170.6, 136.6, 133.8, 133.3, 131.2, 128.3, 127.8, 127.2, 125.9, 125.6, 125.4, 125.0, 123.0, 122.8, 121.0, 118.3, 117.8, 110.9, 109.8, 65.9, 55.4, 54.2, 50.3, 47.2, 46.95, 40.98, 25.0; LC-MS (*m/z*): 485 $[M+H]^+$.

4.45. Protein expression and purification

The N-terminal domain of and *Tb*PEX14 (aa 19–84) were cloned into pETM-11 (EMBL). The plasmids were transformed into *E. coli* BL21.5 ml of the overnight culture was inoculated in 500 ml of the autoinduction medium [32] supplemented with 50 μg of kanamycin. When the cell density (OD600) reached 0.8, the temperature was lowered to 18 °C and the cells were grown overnight. The cells were harvested by centrifugation and dissolved in lysis buffer (50 mM Tris pH 8.0, 300 mM NaCl, 10 mM β-mercaptoethanol, 20 mM imidazole, 10 mg/ml DNAseI, 1 mM AEBSF) and lysed by sonication. The lysates, clarified by centrifugation, were passed over a Ni-NTA agarose resin (Qiagen, Germany) pre-equilibrated with buffer A (50 mM Tris pH 8.0, 300 mM NaCl, 10 mM β-mercaptoethanol, 20 mM imidazole) and the protein of interest was eluted with the same buffer containing 250 mM imidazole. The concentrated eluates were further purified on a Superdex 75 Hiload 16/60 column (GE Healthcare) in phosphate-buffered saline (PBS).

4.46. AlphaScreen assay

AlphaScreen assay was used to derive the inhibition constant (Ki) values for the PEX5-*Tb*PEX14 inhibitors, according to the published protocol [6]. 3 nM N-His-PEX14 was mixed with 10 nM biotinylated PEX5-derived peptide (ALSENWAQEFLA) in PBS supplemented with 5 mg/mL of BSA and 0.01% (v/v) Tween-20.5 μg/mL of streptavidin donor beads and 5 μg/mL of nickel chelate acceptor beads (PerkinElmer) were added to the mixture. The serial dilutions of the inhibitors were prepared in DMSO and mixed while keeping constant the concentration of DMSO (5%; this concentration was shown to have no effect on the assay readout). Apparent binding constants of this system ($K_{d\ L^*T}$) was measured for each experimental condition. This indicates that K_i of an inhibitor can be calculated based on the equation:

$$K_i = \frac{EC_{50}}{1 + \frac{[L_T]}{K_{dL^*T}}}$$

(EC_{50} – median effective concentration measured by AlphaScreen, L_T – Protein concentration, K_{dL^*T} – apparent binding constant in the system at given peptide concentration *T*).

The competition curves were measured using a serial dilution of the inhibitor while keeping the concentrations of all other assay components constant. Data were measured in a quadruplicate. The inhibitor EC_{50} was calculated from the Hill sigmoidal fitting fixing the asymptotes at the maximal assay signal (no inhibitor added) and 0, respectively. The signal was determined according to the bead manufacturer instructions. The data were analyzed using Origin Pro 9.0 [33].

4.47. ^{1}H-^{15}N HSQC NMR assay

Compound **12** was tested using ^{1}H-^{15}N 2D correlation spectra on a Bruker Avance III 600 MHz spectrometer (^{1}H frequency 600 MHz) with a QCI cryoprobe. Samples were made up with 200 μM uniformly ^{15}N-labelled TcPEX14 protein in phosphate NMR buffer (pH 6.5, 20 mM NaCl, 5 mM Na_2PO_4) in water, supplemented with 10% D_2O. Compound **12** was dissolved in DMSO-d_6 and qliquots were added to the test samples at 2.5:1, 5:1 and 10:1 and DMSO-d_6 was added to the reference sample.

4.48. In vitro trypanocidal activity of compounds against T. b. brucei

T. b. brucei bloodstream form (Lister 427, MITat 1.2) parasites were grown in a HMI-11 medium [34] containing 10% fetal bovine serum (FBS) at 37 °C with 5% CO_2. Antitrypanosomal activities of the compounds were tested using resazurin-based 96-well plate assay. Twofold serial dilutions of each compound (10 wells in each row) were prepared in 96-well plates in HMI-11 medium (100 μL/well, quadruplicates). As controls, each row included a well without compound and a well with medium alone. 100 μL of parasite cultures (4×10^3/mL) were inoculated in all wells, except in the well with media alone. Final concentration of parasites was 2×10^3/mL. The plates were incubated for 66 h. Resazurin (25 μL of 0.1 mg/mL in Hanks Balanced Salt Solution) was added to all wells and the plates were further incubated until 72 h timepoint. Reduction of resazurin by living cells was quantified by measuring the fluorescence with a Synergy H1 microplate reader (excitation 530 nm, emission 585 nm). After subtracting the background fluorescence of the well with media alone, percent survival values were calculated by setting the fluorescence of the wells without compound to "100% survival". Nonlinear regression graphs were plotted in GraphPad Software GraphPad Prism 6.04 [35] to yield sigmoidal dose−response curves and half-maximal effective concentration (EC_{50}) values were determined.

4.49. Cytotoxicity of compounds against HepG2 cells

HepG2 (Hepatocyte) cells were seeded in 96-well plates (5000 cells/well in rows B−H) and grown overnight at 37 °C in humidified incubator with 5% CO_2. Compounds were tested in triplicate from 100 to 3.125 μM (twofold serial dilutions, from row H to row C). Row A contained medium alone and served as a negative control. Row B contained cells alone without inhibitors and served as a positive control. Hygromycin B (InvivoGen) was used as a positive control for cytotoxicity. After incubation for 66 h, 25 μL of 0.1 mg/mL resazurin (dissolved in Hanks Balanced Salt Solution HBSS, Sigma) was added to all wells. Plates were further incubated for 6 h. Fluorescence was measured, and the data were processed as described above for the *T. b. brucei* cytotoxicity assay.

4.50. Molecular docking

The structures of the compounds were generated using ChemOffice 17. The library of compounds was prepared for docking generating the 3D models using YASARA ligand preparation protocols. *Tb*PEX14 protein (PDB accession code: 5L87) was prepared for docking using Yasara Structure [36], by removing the cognate ligand, adding missing side chains and missing hydrogens, and generating protonation states using YASARA Structure's built-in "Clean" command. Docking was performed with YASARA implementation of AutoDock VINA [37,38]. The grid box was generated using as reference the 5L87 native ligand present in the *Tb*PEX14 protein structure, using coordinates: *x*-axis = 24.0 Å, *y*-axis = 32.0 Å, *z*-axis = 28.0 Å. Exhaustiveness parameter was set to 24 to fully exploit VINA's multithreading searches generating 16 poses per ligand. Poses were selected by manual inspection according to the fulfillment of the known *Tb*PEX14 ligands' pharmacophore model.

Declaration of competing interest

The authors declare that they have no known competing financial interests or personal relationships that could have appeared to influence the work reported in this paper.

Data availability

Data will be made available on request.

Acknowledgements

This study has been funded by Narodowe Centrum Nauki (grant UMO-2016/23/B/NZ7/03339 to M.D., M.M. and P.M.), Deutsche Forschungsgemeinschaft (grant FOR1905 to M.S. and R.E.) and by Bundesministerium für Bildung and Forschung (grant PEXMED to G.P., M.S. and R.E).

Appendix A. Supplementary data

Supplementary data to this article can be found online at https://doi.org/10.1016/j.ejmech.2023.115587.

References

[1] T. Walter, R. Erdmann, Current advances in protein import into peroxisomes, Protein J. 38 (3) (2019 Jun) 351–362, https://doi.org/10.1007/s10930-019-09835-6.
[2] V.C. Kalel, R. Erdmann, Unraveling of the structure and function of peroxisomal protein import machineries, Subcell. Biochem. 89 (2018) 299–321, https://doi.org/10.1007/978-981-13-2233-4_13.
[3] M.L. Skowyra, T.A. Rapoport, PEX5 translocation into and out of peroxisomes drives matrix protein import, Mol. Cell 82 (17) (2022 Sep 1) 3209–3225.e7, https://doi.org/10.1016/j.molcel.2022.07.004.
[4] Y. Gao, M.L. Skowyra, P. Feng, T.A. Rapoport, Protein import into peroxisomes occurs through a nuclear pore-like phase, Science 378 (6625) (2022 Dec 16), eadf3971, https://doi.org/10.1126/science.adf3971.
[5] R. Ravindran, I.O.L. Bacellar, X. Castellanos-Girouard, Z. Zhang, L. Kisley, S. W. Michnick, Peroxisome biogenesis initiated by protein phase separation, bioRxiv (2022), 508718, https://doi.org/10.1101/2022.09.20.508718, 09.20.
[6] M. Dawidowski, L. Emmanouilidis, V.C. Kalel, K. Tripsianes, K. Schorpp, K. Hadian, M. Kaiser, P. Mäser, M. Kolonko, S. Tanghe, A. Rodriguez, W. Schliebs, R. Erdmann, M. Sattler, G.M. Popowicz, Inhibitors of PEX14 disrupt protein import into glycosomes and kill *Trypanosoma*parasites, Science 355 (6332) (2017 Mar 31) 1416–1420, https://doi.org/10.1126/science.aal1807.
[7] C. Neufeld, F.V. Filipp, B. Simon, A. Neuhaus, N. Schüller, C. David, H. Kooshapur, T. Madl, R. Erdmann, W. Schliebs, M. Wilmanns, M. Sattler, Structural basis for competitive interactions of Pex14 with the import receptors Pex5 and Pex19, EMBO J. 28 (6) (2009 Mar 18) 745–754, https://doi.org/10.1038/emboj.2009.7.
[8] A. Neuhaus, H. Kooshapur, J. Wolf, N.H. Meyer, T. Madl, J. Saidowsky, E. Hambruch, A. Lazam, M. Jung, M. Sattler, W. Schliebs, R. Erdmann, A novel Pex14 protein-interacting site of human Pex5 is critical for matrix protein import into peroxisomes, J. Biol. Chem. 289 (1) (2014 Jan 3) 437–448, https://doi.org/10.1074/jbc.M113.499707.
[9] M. Gopalswamy, C. Zheng, S. Gaussmann, H. Kooshapur, E. Hambruch, W. Schliebs, R. Erdmann, I. Antes, M. Sattler, Distinct conformational and energetic features define the specific recognition of (di)aromatic peptide motifs by PEX14, Biol. Chem. 404 (2–3) (2022 Nov 28) 179–194, https://doi.org/10.1515/hsz-2022-0177.
[10] S. Gaussmann, M. Gopalswamy, M. Eberhardt, M. Reuter, P. Zou, W. Schliebs, R. Erdmann, M. Sattler, Membrane interactions of the peroxisomal proteins PEX5 and PEX14, Front. Cell Dev. Biol. 9 (2021 Apr 16), 651449, https://doi.org/10.3389/fcell.2021.651449.
[11] M. Dawidowski, V.C. Kalel, V. Napolitano, R. Fino, K. Schorpp, L. Emmanouilidis, D. Lenhart, M. Ostertag, M. Kaiser, M. Kolonko, B. Tippler, W. Schliebs, G. Dubin, P. Mäser, I.V. Tetko, K. Hadian, O. Plettenburg, R. Erdmann, M. Sattler, G. M. Popowicz, Structure-activity relationship in pyrazolo[4,3-*c*]pyridines, first inhibitors of PEX14-PEX5 protein-protein interaction with trypanocidal activity, J. Med. Chem. 63 (2) (2020 Jan 23) 847–879, https://doi.org/10.1021/acs.jmedchem.9b01876.
[12] R. Fino, D. Lenhart, V.C. Kalel, C.A. Softley, V. Napolitano, R. Byrne, W. Schliebs, M. Dawidowski, R. Erdmann, M. Sattler, G. Schneider, O. Plettenburg, G. M. Popowicz, Computer-aided design and synthesis of a new class of PEX14 inhibitors: substituted 2,3,4,5-tetrahydrobenzo[F][1,4]oxazepines as potential new trypanocidal agents, J. Chem. Inf. Model. 61 (10) (2021 Oct 25) 5256–5268, https://doi.org/10.1021/acs.jcim.1c00472.
[13] V. Napolitano, P. Mróz, M. Marciniak, V.C. Kalel, C.A. Softley, J.D. Janna Olmos, B. G. Tippler, K. Schorpp, S. Rioton, T. Fröhlich, O. Plettenburg, K. Hadian, R. Erdmann, M. Sattler, G.M. Popowicz, M. Dawidowski, G. Dubin, Structure-based design, synthesis and evaluation of a novel family of PEX5-PEX14 interaction inhibitors against Trypanosoma, Eur. J. Med. Chem. 243 (2022 Dec 5), 114778, https://doi.org/10.1016/j.ejmech.2022.
[14] H. Lu, Q. Zhou, J. He, Z. Jiang, C. Peng, R. Tong, J. Shi, Recent advances in the development of protein-protein interactions modulators: mechanisms and clinical trials, Signal Transduct. Targeted Ther. 5 (1) (2020 Sep 23) 213, https://doi.org/10.1038/s41392-020-00315-3.
[15] D. Valenti, S. Hristeva, D. Tzalis, C. Ottmann, Clinical candidates modulating protein-protein interactions: the fragment-based experience, Eur. J. Med. Chem. 167 (2019 Apr 1) 76–95, https://doi.org/10.1016/j.ejmech.2019.01.084.
[16] Y. Qiu, X. Li, X. He, J. Pu, J. Zhang, S. Lu, Computational methods-guided design of modulators targeting protein-protein interactions (PPIs), Eur. J. Med. Chem. 207 (2020 Dec 1), 112764, https://doi.org/10.1016/j.ejmech.2020.112764.
[17] X. Ran, J.E. Gestwicki, Inhibitors of protein-protein interactions (PPIs): an analysis of scaffold choices and buried surface area, Curr. Opin. Chem. Biol. 44 (2018 Jun) 75–86, https://doi.org/10.1016/j.cbpa.2018.06.004.
[18] S. Algar, M. Martín-Martínez, R. González-Muñiz, Evolution in non-peptide α-helix mimetics on the road to effective protein-protein interaction modulators, Eur. J. Med. Chem. 211 (2021 Feb 5), 113015, https://doi.org/10.1016/j.ejmech.2020.113015.
[19] X. Wang, D. Ni, Y. Liu, S. Lu, Rational design of peptide-based inhibitors disrupting protein-protein interactions, Front. Chem. 9 (2021 May 4), 682675, https://doi.org/10.3389/fchem.2021.682675.
[20] G. Zhang, J. Andersen, G. Gerona-Navarro, Peptidomimetics targeting protein-protein interactions for therapeutic development, Protein Pept. Lett. 25 (12) (2018) 1076–1089, https://doi.org/10.2174/0929866525666181101100842.
[21] P. Tosovská, P.S. Arora, Oligooxopiperazines as nonpeptidic alpha-helix mimetics, Org. Lett. 12 (7) (2010 Apr 2) 1588–1591, https://doi.org/10.1021/ol1003143.
[22] B.B. Lao, K. Drew, D.A. Guarracino, T.F. Brewer, D.W. Heindel, R. Bonneau, P. S. Arora, Rational design of topographical helix mimics as potent inhibitors of protein-protein interactions, J. Am. Chem. Soc. 136 (22) (2014 Jun 4) 7877–7888, https://doi.org/10.1021/ja502310r.
[23] B.B. Lao, I. Grishagin, H. Mesallati, T.F. Brewer, B.Z. Olenyuk, P.S. Arora, In vivo modulation of hypoxia-inducible signaling by topographical helix mimetics, Proc. Natl. Acad. Sci. U. S. A. 111 (21) (2014 May 27) 7531–7536, https://doi.org/10.1073/pnas.1402393111.
[24] F. Tedesco, L. Calugi, E. Lenci, A. Trabocchi, Peptidomimetic small-molecule inhibitors of 3CLPro activity and spike-ACE2 interaction: toward dual-action molecules against coronavirus infections, J. Org. Chem. 87 (18) (2022 Sep 16) 12041–12051, https://doi.org/10.1021/acs.joc.2c01047.
[25] A. Yasgar, A. Jadhav, A. Simeonov, N.P. Coussens, AlphaScreen-based assays: ultra-high-throughput screening for small-molecule inhibitors of challenging enzymes and protein-protein interactions, Methods Mol. Biol. 1439 (2016) 77–98, https://doi.org/10.1007/978-1-4939-3673-1_5.
[26] E.L. Ratkova, M. Dawidowski, V. Napolitano, G. Dubin, R. Fino, M.S. Ostertag, M. Sattler, G. Popowicz, I.V. Tetko, Water envelope has a critical impact on the design of protein-protein interaction inhibitors, Chem. Commun. 56 (31) (2020 Apr 21) 4360–4363, https://doi.org/10.1039/c9cc07714f.
[27] For example, similar scaffold with an N-terminal residue attached to the N-4 atom was used in design of a constrained analog of Leu-enkephalin: K. Shreder, L. Zhang, M. Goodman, Synthesis of a constrained enkephalin analog to illustrate a novel route to the piperazinone ring structure Tetrahedron Lett. 39 (3–4) (1998) 221–224, https://doi.org/10.1016/S0040-4039(97)10530-5.
[28] T. Kan, T. Fukuyama, Highly versatile synthesis of nitrogen-containing compounds by means of nitrobenzenesulfonamides, J. Synth. Org. Chem., Jpn. 59 (8) (2001) 779–789, https://doi.org/10.5059/yukigoseikyokaishi.59.779.
[29] J.R. Parikh, W. von Eggers Doering, Sulfur trioxide in the oxidation of alcohols by dimethyl sulfoxide, J. Am. Chem. Soc. 89 (21) (1967) 5505–5507, https://doi.org/10.1021/ja00997a067.
[30] Y. Hamada, T. Shioiri, New methods and reagents in organic synthesis. 29. A practical method for the preparation of optically active N-protected α-amino aldehydes and peptide aldehydes, Chem. Pharm. Bull. 30 (5) (1982) 1921–1924, https://doi.org/10.1248/cpb.30.1921.
[31] Patent: WO/2007/107545.
[32] F.W. Studier, Protein production by auto-induction in high density shaking cultures, Protein Expr. Purif. 41 (1) (2005 May) 207–234, https://doi.org/10.1016/j.pep.2005.01.016.
[33] OriginPro, 9.0; OriginLab Corporation: (Northampton, MA, USA).
[34] H. Hirumi, K. Hirumi, Continuous cultivation of Trypanosoma brucei blood stream forms in a medium containing a low concentration of serum protein without feeder cell layers, J. Parasitol. 75 (6) (1989 Dec) 985–989.
[35] GraphPad Prism, 6.04; GraphPad Software, Inc: San Diego, CA, USA.
[36] E. Krieger, G. Vriend, YASARA View - molecular graphics for all devices - from smartphones to workstations, Bioinformatics 30 (20) (2014 Oct 15) 2981–2982, https://doi.org/10.1093/bioinformatics/btu426.
[37] G.M. Morris, R. Huey, W. Lindstrom, M.F. Sanner, R.K. Belew, D.S. Goodsell, A. J. Olson, AutoDock4 and AutoDockTools4: automated docking with selective receptor flexibility, J. Comput. Chem. 30 (16) (2009 Dec) 2785–2791, https://doi.org/10.1002/jcc.21256.
[38] O. Trott, A.J. Olson, AutoDock Vina: improving the speed and accuracy of docking with a new scoring function, efficient optimization, and multithreading, J. Comput. Chem. 31 (2) (2010 Jan 30) 455–461, https://doi.org/10.1002/jcc.21334.